CFD Simulation of Reactor Bed for Adsorbed Natural Gas Storage System

by

Wan Ahmad Ammar bin Wan Abd Aziz

(13416)

Dissertation submitted in partial fulfilment of
the requirements for the
Bachelor of Engineering (Hons)
(Mechanical Engineering)

JANUARY 2014

Universiti Teknologi PETRONAS
Bandar Seri Iskandar
31750 Tronoh
Perak Darul Ridzuan

CERTIFICATION OF APPROVAL

CFD Simulation of Reactor Bed for Adsorbed Natural Gas Storage System

By

Wan Ahmad Ammar bin Wan Abd Aziz
(13416)

A project dissertation submitted to the
Mechanical Engineering Programme
Universiti Teknologi PETRONAS
In partial fulfilment of the requirement for the
Bachelor Of Engineering (Hons)
(Mechanical Engineering)

Approved by,

_____

(DR KHAIRUL HABIB)

UNIVERSITI TEKNOLOGI PETRONAS
TRONOH, PERAK
JANUARY 2014

CERTIFICATION OF ORIGINALITY

This is to certify that I am responsible for the work submitted in this project, that the original work is my own except as specified in the references and acknowledgements, and that the original work contained herein have not been undertaken or done by unspecified sources or persons.

_____

WAN AHMAD AMMAR B WAN ABD AZIZ

ABSTRACT

Natural Gas (NG) has emerged as an alternative energy source especially in transportation due to clean burning and have relatively lower price than gasoline. The world awareness toward environmental issues has promoted NG to be future fuel source for the sake of future generations. Even though the current NG technology has not yet convince mankind but still NG receive the overwhelming welcome from global environmentalist. The conventional method of storing and supplying NG is either in the Compressed Natural Gas (CNG) or Liquefied Natural Gas (LNG). However, CNG and LNG had shown some disadvantages throughout its operation. CNG incurs high manufacturing and filling costs and also represents a safety concern while LNG needs specialized equipment for re-gasification. These disadvantages have led to the invention of the adsorbed natural gas (ANG) storage system. The research for ANG has been expending throughout many years and some researcher has produced few design and model for ANG storage system. Nevertheless, there are stills many uncertainties regarding the design and thus need modification and improvement to optimize the ANG storage system. This project is focus on CFD simulation to ANG storage system to analyze the temperature and pressure profiles in the system. The importance of this project is that it can avoid expensive trial and error experiments by defining boundary condition and analyzing all possible output parameters thus, precious cost and time can be save. The major difficulty for this project is less literature has been produce with regard to CFD simulation for ANG storage system so many aspects and uncertainties need to be analyzed and research thoroughly. The impact for this project is to give more insight to the development of ANG technology and indirectly contribute to save the environment.

ACKNOWLEDGEMENT

I would like to take the opportunity to acknowledge and thank everyone that has given me all the supports and guidance throughout the whole period of completing the final year project. Firstly, many thanks to the university and the Final Year Project coordinators that have coordinated and made the necessary arrangements, especially in terms of the logistics, for this study.

I must also acknowledge the endless help and support received from my supervisor, Dr. Khairul Habib throughout the whole period of completing the final year project. His guidance and advices are most appreciated. Apart from that, many thanks to Dr. Mohana Sundaram A/L Muthuvalu, co supervisor that help me from the beginning of the project until its completion. He guided me not only in theory as well as how to deal with technical and non-technical problems. He had much bring me a great strength and support to complete this project successfully.

Finally many thanks to my fellow colleagues for their help and ideas throughout the completion of this study.

Thank you.

Wan Ahmad Ammar bin Wan Abd Aziz
Mechanical Engineering Department

TABLE OF CONTENTS

LIST OF TABLES

LIST OF FIGURES

NOMENCLATURE

A	Adsorption potential [kJ/kg]
C	Adsorption equilibrium uptake [kg/kg]
C_o	Maximum equilibrium adsorption uptake [kg/kg]
C_{eq}	Adsorption equilibrium uptake [kg/kg]
c_p	Specific heat capacity [kJ/kg.K]
E	Adsorption characteristics energy [kJ/kg]
H_{ads}	Heat of adsorption [kJ/kg]
k_o	Equilibrium constant of the Langmuir and Toth isotherm models [1/MPa]
K_{eff}	Overal effective mass transfer coefficient which is function of both equilibrium pressure and temperature [1/s]
$k_s a_v$	Effective mass transfer coefficient which is function of equilibrium pressure [1/s]
n	Index of Dubinin-Astakhov isotherm model
P	Pressure [MPa]
P^*	Equilibrium process pressure [MPa]
R	Universal gas constant [kJ/kg.K]
T	Temperature [K]
T^*	Equilibrium process temperature [K]
t	Time [s] or Heterogeneity parameter of the Toth isotherm model
V	Volume [m^3]
v	Specific volume [cm^3/g]
W	Volumetric adsorption equilibrium uptake [V/V]
W_o	Maximum volumetric adsorption equilibrium uptake [V/V]

Greek

α	Thermal expansion coefficient for the adsorbed phase [K^{-1}]
β	Effective mass transfer coefficient which is function of equilibrium temperature [1/s]
ε	Porosity
ρ	Density [kg/m^3]
θ	Surface coverage
μ	Viscosity [kPa.s]
ψ	Darcy's law coefficient [m^2/kPa.s]

Subscripts

a, adsorbed	Adsorbed phase
ac	Activated carbon
b	Adsorbent bed or boiling point
bed	Adsorbent bed
cri	Critical point
charge	Charge process
discharge	Discharge process
f	Liquid phase
g	Gaseous phase
s, solid	Solid adsorbent
sat	Saturation point
t	Total
vapor	Vapor phase

CHAPTER 1

INTRODUCTION

1.1 Background of Study

Increase in environmental awareness and instability in the oil markets have stimulated research for alternative transportation fuels. One alternative to gasoline is natural gas, which consists primarily of methane (85-95%) with minor amounts of ethane, other higher-order hydrocarbons, nitrogen, and carbon dioxide [1]. Natural gas has emerged as a promising alternative since it produces less carbon emission and provides clean combustion hence lowers exhaust pollution compared to gasoline for transportation. According to the EPA, compared to traditional vehicles, vehicles operating on compressed natural gas have reductions in carbon monoxide emissions of 90 to 97 percent, and reductions in carbon dioxide emissions of 25 percent. Nitrogen oxide emissions can be reduced by 35 to 60 percent, and other non-methane hydrocarbon emissions could be reduced by as much as 50 to 75 percent [2]. The conventional method of storing and supplying Natural Gas (NG) are the compressed natural gas (CNG) and liquefied natural gas (LNG) storage system. The compressed form of natural gas known as (CNG) is stored at high pressures up to 30 MPa while the liquefied natural gas (LNG) is stored at cryogenic temperature (–163 °C). However, CNG and LNG had shown some disadvantages throughout its operation. CNG incurs high manufacturing and filling costs and also represents a safety concern while LNG needs specialized equipment for re-gasification [3]. These disadvantages have led to the invention of the adsorbed natural gas (ANG) storage system. The ANG storage system provides high energy density but operates at much lower pressure (usually 2 to 4 MPa) than the CNG method. Also, the ANG system does not require costly cold energy to store gas in the liquid phase as does LNG. ANG storage systems have been intensively studied in recent years [4]. On the other hand, ANG storage system has attracted considerable attention as a possible alternative to the CNG and the LNG methods for energy storage and transportation purposes [5].

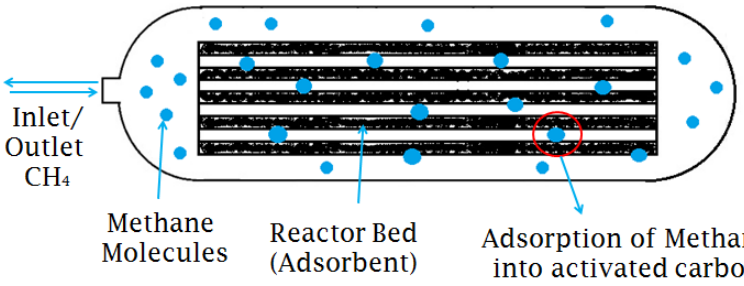

Figure 1.1 Cross-Section of ANG Storage System

ANG storage system is a technology in term of method for storing natural gas by using adsorption application via porous adsorbent. Referring to the Figure 1.1 above, the adsorbate which is the methane gas is pressurized and stored in a vessel or tank which was compacted with adsorbent. The pores of the adsorbent will captured the gas molecules due to the strong attractive surface forces known as van der Walls forces. This process is called adsorption as the gas molecules will be stored in the pores of adsorbent. Figure 1.2 below illustrated more clearly the adsorption process that occurs at the pores of adsorbents. The main advantage of adsorption process is that it operates at low pressure and mild temperature.

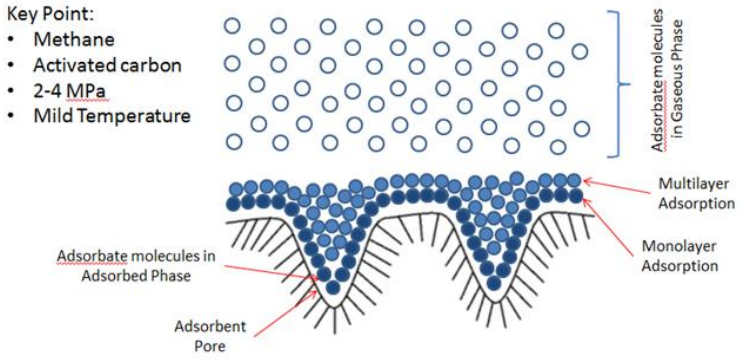

Figure 1.2 Adsorption mechanisms at the pores of adsorbent

1.2 Problem Statement

Natural gas has become a fuel of great industrial interest mainly because of its inherent clean burning characteristics [6]. With regard the current environmental issue mainly global warming, many countries have taken the step by promoting Natural Gas Vehicle (NGV) in order to contribute and help saving the earth for future generation. Now days, there are two commercialized natural gas storage system; Compressed Natural Gas (CNG) storage system currently being implemented in the transportation sector and Liquefied Natural Gas (LNG) storage system currently being focused on providing energy for a certain location. The CNG storage system requires high pressure up to 30 MPa; which means a large pressure vessel needs to be used and also represents safety concerns. Thus, the large pressure vessel is not preferable to be placed in a natural gas vehicle (NGV) using the natural gas as fuel or other location that has limited space. In terms of safety, high pressure and temperature operation of CNG could create fire at a fast rate or explosion. On the other hand, LNG storage system requires very low temperature (approximately 112K) which requires specialized container design and refueling procedures as cryogenic temperature is involved thus require high cost for the fabrication of LNG storage system [3]. Adsorbed natural gas (ANG) storage system is an alternative for CNG and LNG storage system. The main advantages of using ANG storage system, it operates at low pressure (2 to 4 MPa) and the temperature used is near atmospheric temperature storage or mild temperature [3]. However, improvements still need to be done since its storage capacity is less than CNG storage system when it comes to higher pressure because ANG storage will reach equilibrium at low pressure. The developments of mathematical modeling and computational method have led to the invention of design modeling and simulation software which can be used to analyze the uncertainty and possible outcomes for certain design before being fabricate. Computational Fluid Dynamics (CFD) is a computer-based mathematical modeling tool which can be considered the consolidation between theory and experiments in the fields of fluid flow and heat transfer. This project will be using CFD simulation to analyze the model of ANG storage system by the means of temperature and pressure profiles.

1.3 Objectives and Scope of Study

1. To study the effect of different designs for ANG storage reactor bed system toward the adsorption of methane gas.
2. To analyze the pressure and temperature distributions at the reactor bed of ANG storage system due to the adsorption of methane gas.

In terms of the scope of study, the reader would be expecting some basic principles of adsorption engineering in the early stages and get the general ideas on how adsorption works in a natural gas storage system. After that, many equations and calculations will be involved. Next is the modeling the ANG system followed by set boundary condition for the design before performing mesh generation of the model. Then input and output parameter will set upon performing the simulation.

CHAPTER 2

LITERATURE REVIEW

2.1 Adsorbed Natural Gas (ANG) Storage System

Adsorbed natural gas (ANG) is a technology in term of method for storing natural gas by using adsorption application via porous adsorbent. ANG can be considered as an alternative because it provides higher storage capacity operating at lower pressure (2 to 4 MPa) and at room temperature [3]. In ANG storage system, the methane gas which is the adsorbate is pressurized and stored in a vessel or tank which was compacted with activated carbon or so called adsorbent. Based on the adsorption principles, the pores of the adsorbent will captured the gas molecules due to the strong attractive surface forces known as van der Walls forces. The molecular distances inside the pores of the adsorbent are much shorter than in the gaseous phase for similar pressure and temperature conditions and thus the adsorbate density in adsorbed phase becomes liquid-like [7]. It is found that activated carbons with average pore diameter of less than 20 Å can adsorb gas in an amount which is proportional to its pore volume [8]. Activated carbons with surface areas > 3000 m^2/g and micropore volumes > 1.5 cm^3/g are now commercially available, which are taking ANG closer to viability [9]. The application of adsorbed natural gas (ANG) can be divided into three main categories, on-board fuel storage, mobile tanker supply and large-scale natural gas storage [10]. Besides that, the advantages of ANG are the safety is higher than CNG (7-40 bar) and can be operate at mild temperature. Moreover it can provide high volumetric capacity and does not need extensive inlet and outlet compression (like CNG) is required.

2.1.1 Activated Carbon (Maxsorb III)

Activated carbons are the microporous carbonaceous adsorbents which were discovered back in the 1600 B.C. when wood chars were used as medicines in Egypt. Activated carbons are produced in three forms; which are granular, pelletized, and powdered forms. Depending on the precursor materials and the manufacturing processes, there are four types of activated carbons available for various applications. They are powdered activated carbon (PAC), granular activated carbon (GAC), carbon molecular sieve (CMS), and activated carbon fiber (ACF) [7]. All of them have been reported in the literature and investigated for possible use in ANG storage application. However, calculations made are based on using powdered Maxsorb III. The powdered type activated carbon, which is known as Maxsorb III, was supplied by Kansai Coke and Chemicals Co. Ltd., Osaka, Japan with a stated surface area of 3140 m^2/g and a micropore volume (υ_μ) of 1.7 cm^3/g. It has a mean particle diameter of 72 μm, an ash content of no more than 0.1%, and moisture of no more than 0.8 % [9]. Maxsorb III is selected because it has the highest surface area and the highest pole volume compare to other activated carbon on the market. There was a study done on the adsorption of n-butane on pitch based Maxsorb III at temperatures ranging from 298 to 328 K and at different equilibrium pressure between 20 and 300 kPa have been experimentally measured by a volumetric technique [9]. Table 2.1 shows the porous properties such as, the Brunauer, Emmett and Teller (BET) surface area, pore size, pore volume, porosity, and skeletal density [10]. The scanning electron microscopic (SEM) photograph of Maxsorb III at 1000 magnification ratio is also shown in Figure 2.1 [11].

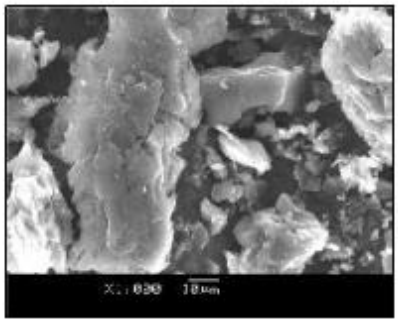

FIgure 2.1: Scanning electron micrographs (SEM) photograph of Maxsorb III sample at 1000 magnification ratio [3]

Table 2.1: Porous properties on Maxsorb III

Porous properties of Maxsorb III	
Brunauer, Emmett Teller (BET) Surface Area (m^2/g)	3276
Micropore volume (ml/g)	1.70
Total pore volume (ml/g)	2.01
Average pore diameter (Å)	20.85
Skeletal density (kg/m^3)	2200
Apparent density (g/ml)	0.31
Residual heat (%)	0.1
pH (-)	4.1
Mass reduction during preparation from carbon (%)	0.8
Average particle diameter (µm)	72
Mean pore diameter (nm)	2.008

It is also observed that the H_{ads} values are higher for the Chemviron sample and lowest for the Maxsorb III sample in tune with *E* values as listed in Table 2.2. This can be another reason for the Maxsorb III sample to be used in the ANG storage system to lessen the thermal load in temperature management.

Table 2.2 Adsorption parameters for the D-A isotherm (*W0*, *E* and *n*) model with the adsorbed phase volume correction [3]

Parameters	Maxsorb III		ACF (A-20)		Chemviron	
↓ *a* (1/K) →	0.0025	1/T	0.0025	1/T	0.0025	1/T
W_0 (cm^3/g)	1.211	1.618	0.717	0.941	0.407	0.504
E 9J/mol)	5835	5258	6198	5641	8684	8258
n	1.46	1.33	1.51	1.37	1.86	1.70
Error of Regression (%)	2.5	1	1.7	2.2	1.8	4.1

2.1.2 Methane

Methane, the main component of natural gas, has a superior octane number than other fuels. However, at the normal conditions of temperature and pressure, it is a supercritical gas and thus has low energy density. The purity grade of the sample used was 99.9995 % of CH_4 with the supplier stated impurity levels as follows: N_2 < 5 ppm, CO < 1 ppm, O_2 < 1 ppm, OHC < 0.5 ppm, C_2H_6 < 1 ppm, and H_2O < 1 ppm [9].

2.2 Adsorption

2.2.1 Definition and Concept

Adsorption can be defined in many ways. Several books, websites, published papers and other references show that adsorption can have many definitions but still in the same concept. Adsorption means the process involving separation of a substance from one phase accompanied by its accumulation or concentration at the surface of another [12]. Generally, we can understand that adsorption is a process that occurs when a gas or liquid accumulates on the surface of a solid or a liquid is called adsorbent, forming a molecular or atomic film called the adsorbate. The term adsorption is different from absorption, in which a substance diffuses into a liquid or solid to form a solution. Another term called ‘desorption’ is simply the reverse phenomenon of adsorption. Adsorption is operative in most natural physical, biological, and chemical systems, and is widely used in industrial applications. Normally adsorption can be classified into physical adsorption and chemical adsorption.

2.2.2 Adsorption Mechanisms

Adsorption can be classified into two types of mechanisms; which are physical adsorption and chemical adsorption. For the physical adsorption process, the adsorbate (gas or liquid) molecules are attracted onto the surfaces of the adsorbent (solid) by the van der Waals forces. Most of the adsorbate molecules are held at the micropores and some extent at the mesopores of the adsorbent [13]. Since the phenomena are physical in nature, physical adsorption process can be reversible. Physical adsorption is also an exothermic process since heat is released during the adsorption and desorption process. This is due to the change in energy level of the adsorbate molecules between gaseous and adsorbed phases [7]. Another type of adsorption is chemical adsorption. This process involves reactions between adsorbate and adsorbent thus resulting in chemical bond formation [14]. On the other hand, this process is not completely reversible. ANG system is reversible because the process can be desorb by altering the pressure and temperature.

2.2.3 Adsorption Equilibrium

During the adsorption process of adsorbate onto the adsorbent surfaces, adsorbate molecules will gather and both the adsorbate and adsorbent will reach an equilibrium state. The amount of adsorbate adsorbed onto the adsorbent surface at equilibrium condition is known as the equilibrium adsorption uptake, C_{eq} and it is a function of equilibrium pressure (P^*) and equilibrium temperature (T^*), i.e. $C_{eq} = f(P^*, T^*)$. When the temperature is constant, the change in equilibrium adsorption uptake against the equilibrium pressure is called the adsorption isotherm, i.e. $Ceq = f(P^*, T^*)$ at T. The adsorption isotherm can be demonstrated as in Figure 2.2 [3].

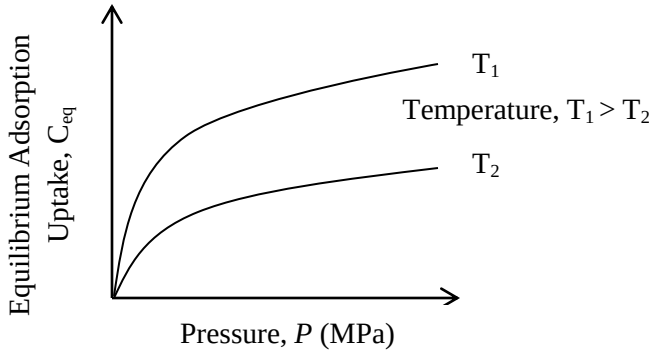

Figure 2.2 Adsorption Isotherm, $C = f(P)$ at T [3]

In order to design any system that involves adsorption processes, the adsorption isotherm of an adsorbate/adsorbent pair is one of the important characteristics that have to be considered. Therefore, the measurement of adsorption isotherms of methane on activated carbon Maxsorb III is important to obtain the storage capacity of the ANG storage system. There are different techniques that can be implemented to measure the adsorption isotherms, which are mainly volumetric, gravimetric and gas flow techniques [7]. The volumetric is the most common technique used because of its simplicity and accuracy. Adsorption equilibrium which consist of mathematical forms are used together with isotherm models to describe adsorption isotherms. A number of adsorption equilibrium models are found in the literature to describe the adsorption isotherm data for different adsorbate-adsorbent pairs [15]. There are three different adsorption isotherm models that normally used by researcher, namely those of Langmuir, Tóth and Dubinin-Astakhov.

2.3 Computational Fluid Dynamic (CFD)

Computational Fluid Dynamics (CFD) is a computer-based mathematical modeling tool which can be considered the consolidation between theory and experiments in the fields of fluid flow and heat transfer [16]. CFD simulation is important tools for the design and optimization of chemical process. The main purposes are to avoid expensive trial and error experiment and to give insight for further improvement of the design since it can approximately predict fluid flow, heat transfer and also chemical reaction in complex system. Nevertheless it still cannot provide absolute result since there are still uncertainties to the system. Apart from that, CFD is used to construct design parameter prior to any physical prototype and also can be perform using different operating condition. Until today, CFD have been proven significant to various range of process applications such as polymerization reactors, fluidized beds, bioreactors, environmental issues and several more [17]. The calculations of CFD are based on Navier-Stokes equations which are a set of partial differential equations that cannot be solved analytically except in a limited number of cases. These equations were come out from the combination of simple fundamental governing equations of fluid dynamics: the conservation of mass, momentum and energy. However, an approximate solution can be obtained using a discretisation method that approximates the partial differential equations by a set of algebraic equations. The techniques that used to perform this discretisation are the finite volume method, the finite element method and the finite difference method [16].

CHAPTER 3

METHODOLOGY

The research methodology for this project is mostly done by experienced learned from internship project, self-reading, and self-exploration on various matters related to technical knowledge and tools required to develop simulation to analyse the temperature and pressure changes in ANG Storage Tank. This chapter consists of (1) research methodology, (2) gantt chart, (3) key milestone, and (4) tools and equipment.

3.1 Research Methodology

Figure 3.1 illustrate the project flow chart for this project. For the first step in this project, preliminary studies on adsorption of methane by activated carbon have been done to determine the possible variables that can be consider in this project. From this preliminary studies, base case for this project have been determine, where this simulation will focusing on reactor bed of ANG Storage Tank. All the information obtains in this step will be used in development of model.

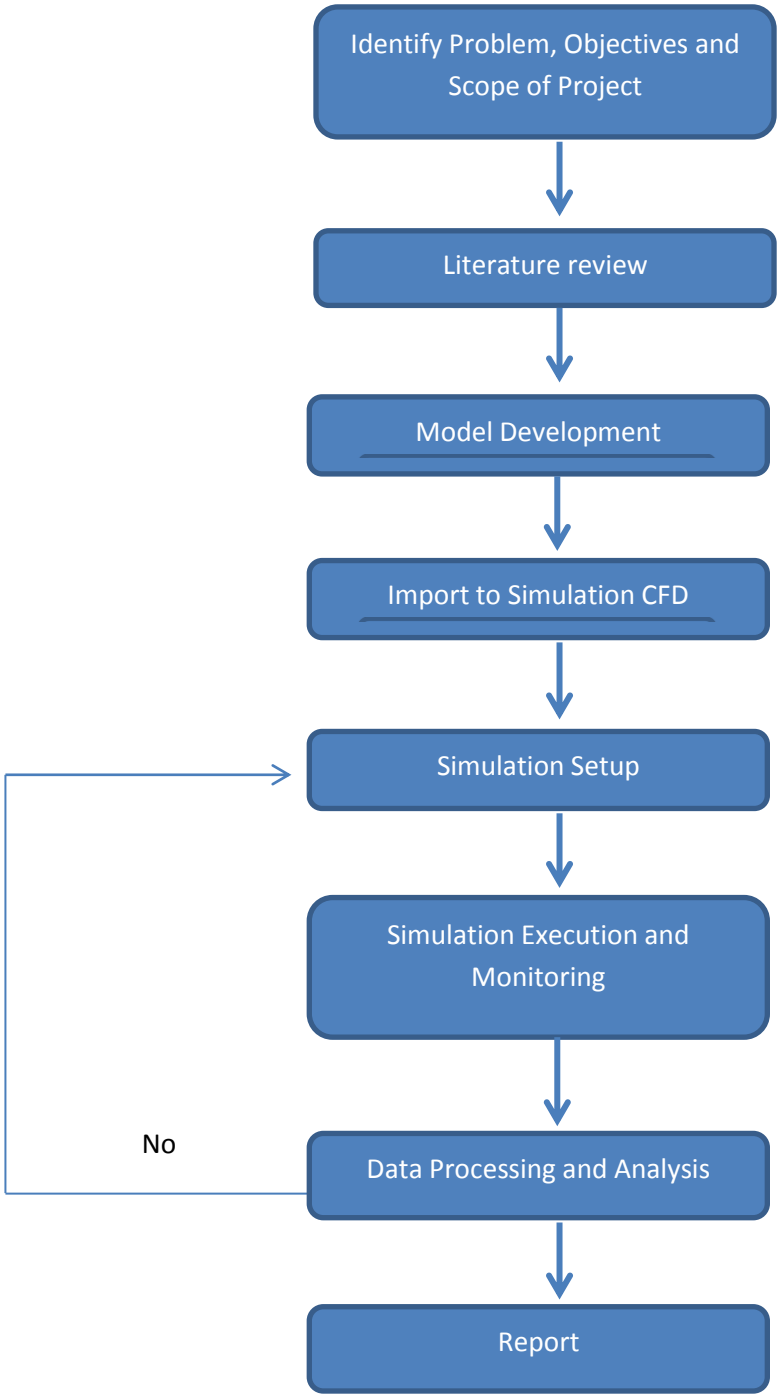

Figure 3.1: Project Flow Chart

The problem for the project should be identified first. After identifying the problem, then the objectives of the project can be determined, which to develop model for ANG storage system and to perform simulation by using CFD. Another objective is to analyze the ANG storage system in term of temperature and pressure profiles based on CFD simulation.

Conduct a research regarding the current technology of ANG storage tank, characteristic of adsorption and also previous study about ANG. Gather the important information regarding those techniques based on the previous study and experiment to carry out the project. Produce a literature review based on the information obtained.

Produce several designs of ANG Storage Tank with different reactor bed to be analyse. The designs supposed to start with simple design and later on proceed with more complex design. All related parameters should be determine to increase the accuracy of the results.

The new design of ANG storage tank will be simulate using the ANSYS software and collect the temperature and pressure distribution data. If the simulation part is fail to simulate, so step 3 should be repeated. After simulating all the new design of ANG reactor bed, the result and data should be recorded.

Evaluate and analyze the data by comparing the results that been recorded based from the simulation. Compare the temperature and pressure distribution between few designs. Study the effect of baffle plate in ANG Storage Tank. Specify the design of the reactor bed that have the best temperature and pressure distribution.

Prepare final report to conclude the finding about temperature and pressure profile of ANG reactor bed. Produce some recommendations towards the project so that it can be improves and obtain better result in enhancing the adsorption capacity for activated carbon.

3.2 Gantt chart and Key Milestones for FYP 1

No	Detail/Week	1	2	3	4	5	6	7		8	9	10	11	12	13	14
1	Selection of Project Topic								Mid-semester break							
2	Preliminary Research Work															
3	Preliminary Design Stage															
4	Submission of Extended Proposal															
5	Estimation of Project Performance															
6	Proposal Defence															
7	Modeling Stage															
8	Preliminary Simulation Stage															
9	Submission of Interim Draft Report															
10	Submission of Interim Report															

❖ Milestone
Progress

Table 3.1: Gantt Chart & Key Milestone FYP 1

3.3 Gantt chart and Key Milestones for FYP 2

No	Detail/Week	1	2	3	4	5	6	7		8	9	10	11	12	13	14
1	Analysis of Preliminary Results								Mid-semester break							
2	Preparing Progress Report															
3	Final Simulation Stage Using Ansys															
4	Submission of Progress Report															
5	Analysis of Final Results															
6	Preparing Final & Technical Report															
7	Submission of Dissertation (Softbound Copy)															
8	Submission of Technical Paper															
9	Oral Presentation Stage															
10	Submission of Dissertation (Hardbound Copy)															

Table 3.2: Gantt Chart & Key Milestone FYP 2

3.4 Tools Required

ANSYS Fluent software is commonly employed for computational fluid dynamic (CFD) simulations in complex geometries. It is ideally suited for both Newtonian and non-Newtonian fluid-flow simulations. This software is also able to provide complete mesh flexibility including the ability to solve flow problems. ANSYS Fluent software is required in this project to simulate the ANG Storage Tank model that will be model first using CATIA software. The simulation result from this software will be used to analyse the temperature distribution and pressure changes at the reactor bed of ANG Storage Tank.

CHAPTER 4

ADSORPTION CHARACTERISTICS

4.1 Adsorption Isotherms

The analysis of the equilibrium adsorption isotherms data are important to study the adsorption capacity and equilibrium coefficient for adsorption, also it is important in developing accurate data that could be used for adsorption design purpose. Three different isotherm models, those of Langmuir, Tóth and Dubinin-Astakhov, have been used to correlate the equilibrium uptake values. The Langmuir isotherm is the simplest theoretical model for monolayer adsorption which was developed from either kinetic derivation or thermodynamic derivation [13]. Much literature has been produce for Langmuir isotherm in microporous solids such as adsorption of methane in activated carbon. This model is applied to homogeneous sorption [18], [19]. This model is developed by assuming that the forces of interaction between adsorbed molecules are negligible, fixed number of accessible sites are available on the adsorbent surface in which these sites are energetically equivalent and once an adsorbate molecule occupies a site no further adsorption takes place [13], [19]. It presumes a homogeneous surface of the adsorbents where the adsorption energy is constant over all sites. This model also assumes that the adsorption on the adsorbent surface is localized and each site can accommodate only one molecule or atom [20]. The Langmuir model has limitations to fit uptake data at high pressure and for material heterogeneity. The Tóth model is commonly used for heterogeneous adsorbents such as activated carbon because of its correct behavior at both the low and high pressure ends and possesses the correct Henry-law-type behavior [20]. Dubinin and Astakhov proposed the model for adsorption of vapors and gases onto non-homogeneous carbonaceous solids with a wider pore size distribution [20]. This D-A model is allowed for the surface heterogeneity and can be extended to the high pressure ranges. On top of that, Dubinin–Astakhov adsorption

isotherm represents the experimental data well and in the same time provides the heterogeneity parameter of the material which is an important adsorbent physical parameter as well as the adsorption energy [21].

4.1.1 Dubinin-Astakov Adsorption Isotherm Model

The Dubinin-Astakhov (D-A) model assumes that adsorption of vapors and gases onto non-homogeneous carbonaceous solids with a wider pore size distribution. The model is also suited for surface heterogeneity and used in high pressure ranges. The D-A model is shown as [25]

$$W = W_0 [-(A/E)^n] \tag{4.1}$$

where A is the adsorption potential, W is the amount of volumetric equilibrium adsorption uptake, W_o is the maximum volumetric equilibrium adsorption uptake, E is the characteristic energy of the adsorption system and n is the structural heterogeneity parameter. Since adsorption potential can be refer as

$$A = RT \ln(P_{sat}/P) \tag{4.2}$$

Thus, equation 4.2 is changed to

$$C = (W_o / v_a) \exp\left[-\{(RT/E) \ln (P_{sat}/P)\}^n\right] \tag{4.3}$$

Then, to calculate the adsorbed phase specific volume, v_a and saturated pressure, P_{sat}, they are estimated using the following sequences [26].

$$v_a = {}_{\mathrm{b}} \exp [\alpha (T - T_{\mathrm{b}})] \tag{4.4}$$

where v_b is the specific volume of liquid at boiling temperature, T_b and α is the thermal expansion coefficient assume as 0.0025 K^{-1} and [27]

$$P_{sat} = (T/T_{cri})^2 P_{cri} \quad (4.5)$$

where T_{cri} and P_{cri} are the critical pressure and temperature of methane. All the parameters for Dubin-Astakhov model can be referred in Table 4.1 [23].

Table 4.1: Adsorption parameters for Dubinin-Astakhov model

Parameters	Value
W_0 , (m^3/kg)	2.193 x 10^{-3}
E, (kJ/kg)	328.625
n	1.33
A, (K^{-1})	1/T

For Dubinin-Astakhov model, using all of the equations and adsorption parameters given above, Figure 4.1 represents the adsorption uptake of methane onto Maxsorb III.

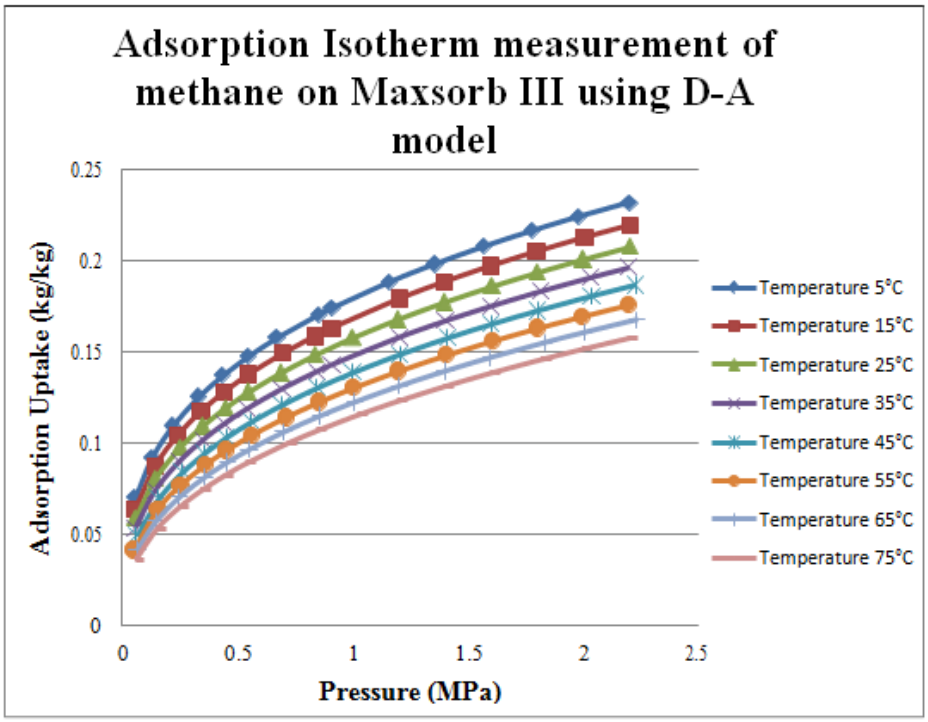

Figure 4.1: Adsorption isotherms of methane onto Maxsorb III using D-A model

From Figure 4.1, it can be seen that at temperature 5^{o}C give the highest adsorption uptake and it decreasing as the temperature increases under certain pressure variation. The highest amount of adsorbate accumulates onto the adsorbent surface is represent by adsorption uptake. Based on D-A isotherm model, the adsorption occur highest at lower temperature. On the other hand, other scholars also mentioned that D-A isotherm model is more appropriate for methane onto Maxsorb III compared to Langmuir and Toth models due to the accountability of the heterogeneity parameter at higher pressures and the consideration of the adsorbed phase volume correction as proposed by Rahman [23].

4.2 Adsorption Kinetics

Adsorption kinetics controlled the diffusion process of the adsorbate molecules into the pores of adsorbent. The porous structure of the adsorbent and the adsorption conditions, such as temperature and concentration range will affect the mechanism of the diffusion process [13]. In adsorbent particles with bidispersed pore structures, such as activated carbon, macropores usually act as a path for the adsorbate molecules to reach the micropores of the adsorbents and thus, the overall diffusion properties will be used to determine the adsorption rate [7]. The measurement of the adsorption kinetics for the working pair that is used in that system is necessary as the performance of an adsorption system depends on both the adsorption capacity and adsorption rate [3]. Adsorption kinetics is described using Linear Driving Force (LDF) model [22] or pseudo-first order reaction model [23] where the rate parameters of the kinetics model are evaluated through regression of the transient adsorption uptake data. The linear driving force model (LDF is a simplified expression of the intra-pellet diffusion equation at which the uptake rate of the adsorbate is linearly proportional to the difference between the equilibrium uptake, C_{eq} and the instantaneous uptake, $C(t)$ [7]. However, this correlation is only valid for isothermal adsorption at which the temperature change of the adsorbent is neglected during the adsorption process. In addition, this phenomenon can only be achieved if there is small change of the adsorbate concentration [3]. In the recent study,

the heat effects associated with adsorption are comparatively large and the adsorbent temperature rises during the adsorption process. Therefore, a non-isothermal kinetics model is employed to represent the adsorption kinetics of methane vapor [24]. Furthermore, the sudden change of the adsorbate concentration in the adsorption cell at the beginning of the adsorption process also contributes to this modified kinetics model.

The linear driving force model (LDF) is used to calculate the adsorption kinetics. It is a simplified expression of the intra-pellet diffusion equation at which the uptake rate of the adsorbate is linearly proportional to the difference between the equilibrium uptake and instantaneous uptake, *C(t)* as proposed by Loh et al. [28]

$$dC/dt = k_s a_v [C_{eq} - C(t)] \tag{4.8}$$

where $k_s a_v$ is the effective mass transfer coefficient and it is the function of adsorbate concentration. Nevertheless, equation 4.8 can be simplified by including the overall effective mass transfer coefficient which is function of both equilibrium pressure and temperature, K_{eff}, as expressed as the following relation [28]

$$dC/dt = k_{eff} [C_{eq} - C(t)] \tag{4.9}$$

where

$$k_{eff} = k_s a_v \; x \; f(P) + \beta \; x \; f(T) \tag{4.10}$$

Referring to equation 4.10, *f(P)* is the pressure profiles and *f(T)* is the temperature profiles. However equation 4.9 will reduces to the original LDF model if the effects of pressure and temperature are significant. After rearranging and integrating equation 4.9, it can be as

$$-ln [C_{eq} - (t)] = K_{eff} + constant \tag{4.11}$$

and using initial condition at t = 0, C(t) = 0, the constant in the above equation becomes ln(C_{eq}) which implies

$$\frac{C_{eq} - C(t)}{C_{eq}} = exp(-K_{eff} t) \tag{4.12}$$

Rearranging equation 4.12, the instantaneous can be expressed as

$$C(t) = C_{eq}[1 - \exp(-K_{eff}t)] \tag{4.13}$$

Table 4.4 gives all of the adsorption parameters needed to calculate the adsorption kinetics [23].

Table 4.2 : Adsorption parameters for adsorption kinetics

Parameters	Values
Effective mass transfer coefficient, $k_s a_v$ (s^{-1})	0.988 – 0.912(P*)
Effective mass transfer coefficient, β (s^{-1})	0.54

In equation 4.10, *f*(P) and *f*(T) represents the pressure and temperature profiles of the adsorbent during the kinetics process at equilibrium temperature of 303K and 0.91MPa. In order to get the values of *f*(P) and *f*(T), we can refer to Rahman; where Figures 4.2 and 4.3 show the temperature and pressure profiles obtained from his study [23].

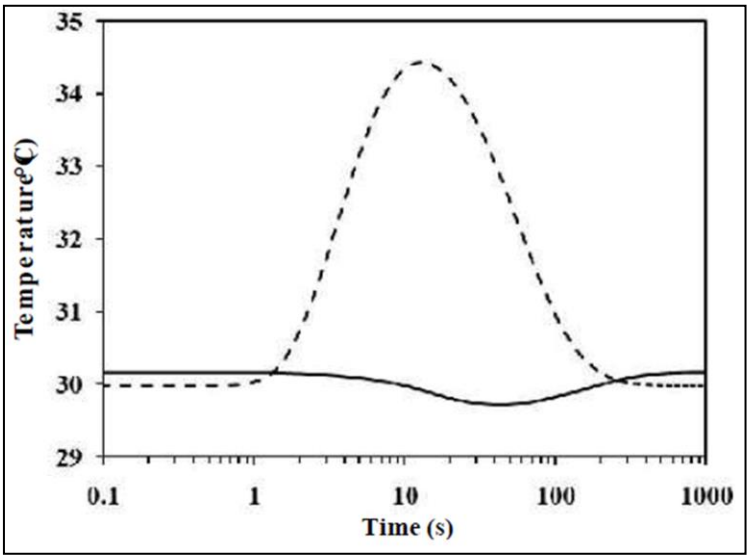

Figure 4.2 : Adsorbent (dashed line) temperature [3]

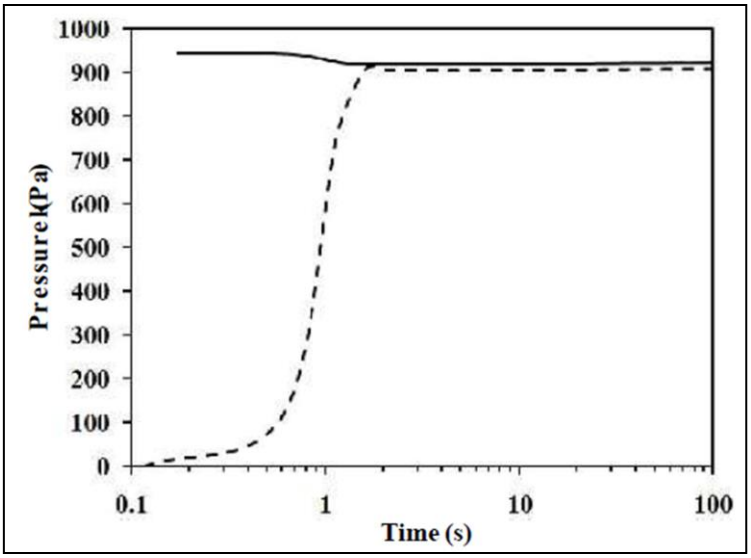

Figure 4.3 : Adsorbent (dashed line) pressure profiles [3]

From Figures 4.2 and 4.3, we will able to calculate the overall effective mass transfer coefficient, K_{eff} as well as using the adsorption parameters in Table 4.4. The graph gained from the calculation is shown in Figure 4.4. The pressures used are 0.21, 0.43 and 0.91 MPa and temperatures at 278K, 288K and 303K

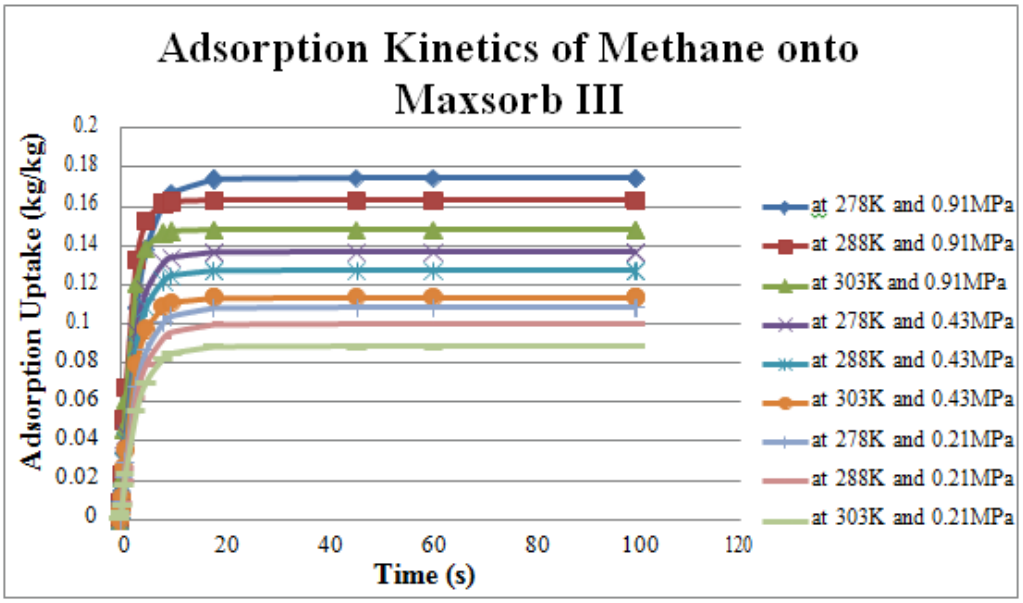

Figure 4.4: Adsorption kinetics of methane onto Maxsorb III

Figure 4.4 shows that the kinetics present an increase of adsorption uptake for methane until it reaches equilibrium. As explained by Loh [29], the possible phenomenon is that the increase of uptake values are mainly due to the charging of the adsorbate into the adsorption cell at high pressures; that is the adsorbate molecules are "rush" into the adsorption cell and they adsorbed onto the solid adsorbent surfaces. As the process continues, heat of adsorption will be released and increase the temperature of the adsorbent. Then, adsorbed molecules are desorbed due to the temperature increased the adsorbent reaches the predetermined temperature and hence reaches equilibrium uptake.

4.3 Heat of Adsorption

Another important characteristic of adsorption is the heat of adsorption. The evaluation of adsorbed phase thermodynamic quantities, such as heat of adsorption, specific heat capacity, internal energy, enthalpy and entropy, are essential for thermodynamic analysis of any adsorption system [3]. Until today, there are many literature been produce relating to the heat of adsorption. The Langmuir and Tóth models provide a constant value for the heat of adsorption (H_{ads}) considering homogeneous surface structure of the adsorbents. However, the heat of adsorption (H_{ads}) becomes function of uptake and temperature when the adsorbent is heterogeneous in surface structure [20].The values of the heat of adsorption ($H_{ads)}$ can be evaluated from the isotherm data using the Clausius-Clayperon equation that assumes the ideal gas behavior of the adsorbate [25]; [26]. In addition, the expression for (H_{ads}) have been derived considering the non-ideality of the gaseous phase of the adsorbate and added a correction term along with the Clausius-Clayperon equation [27]. In the adsorption process, the adsorbate molecules are more stabilized on the adsorbent surface than in the gaseous phase and it is because of the reduction in energy level of the adsorbate molecules that accumulate in the pores of adsorbent with a phase transformation. However the thermal effect is being produce as the result of adsorption/desorption process thus, an effective cooling/heating

arrangement has to be installed to enhance the charge and discharge processes of an adsorptive gas storage system [3].

The values for heat of adsorption for both Langmuir and Toth models are constant and provided considering homogeneous surface structure of the adsorbents. However, heat of adsorption is changing with temperature and pressure when considering heterogeneous in surface structure. Therefore, we can use the isotherm data for these estimations. The Clausius- Clayperon equation in expanded using D-A isotherm model using $\alpha = 1/T$ is used in this calculation [30].

$$H_{ads} = 2RT + E[(ln\frac{W_o}{v_a})^{1/n} + \frac{1}{n}(ln\frac{W_o}{v_a})^{1\text{-}n/n}] \quad (4.14)$$

The adsorption parameters (W_o, v_a, n, E) used in equation 4.14 can be referred back to Table 4.3. Only the temperatures of 298K, 323K and 348K were used for the calculation.

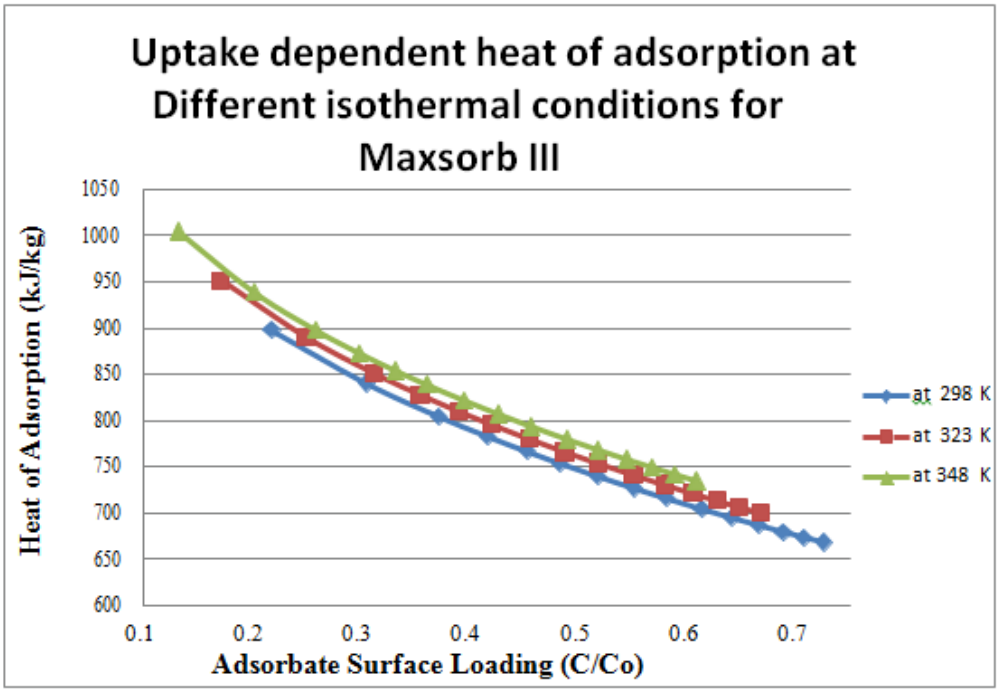

Figure 4.5 Uptake dependent heat of adsorption at different isothermal conditions

As we can see from Figure 4.5, the graph plotted shows the heat of adsorption is decreasing as the adsorbate surface loading increases. Besides that, we can also see that lower temperature shows lower heat of adsorption. To explain this, the adsorbent has many pore sizes, from the biggest to the narrowest. As the adsorbate molecules got attracted to the pores due to van der Waals forces, the adsorbate molecules will go for the narrowest pore size and the energy level is very high; which explains using higher temperature will resulted in higher value for heat of adsorption. After that, as the all of the narrowest pores of the adsorbent have been filled, the adsorbate molecules will start to fill the bigger to the biggest pore size and will require less energy compared to filing the narrower pore size; which explains the decrease in heat of adsorption in Figure 4.5.

CHAPTER 5

SIMULATION FOR REACTOR BED OF ANG STORAGE SYSTEM

`

5.1 Design Development

The next step in this project is to develop and propose the designs of ANG Storage Tank in order to analyse the characteristics and behaviors of certain parameters such as temperature cannot give accurate results since there are many assumptions that have to be made in order to set the boundary condition and also the parameters required to run the simulation. In order to get more accurate and variety results, the author is planning to propose a few more design with different assembly inside the tank. Nevertheless, the design cannot be too complicated as it will require a longer time for simulation. The figure 5.1.1 below is the benchmark model that has been developed by Rahman 2011 in his study about ANG storage system. The author believed that it is crucial to develop a benchmark to compare and validate the results and findings based on previous studies that have been made.

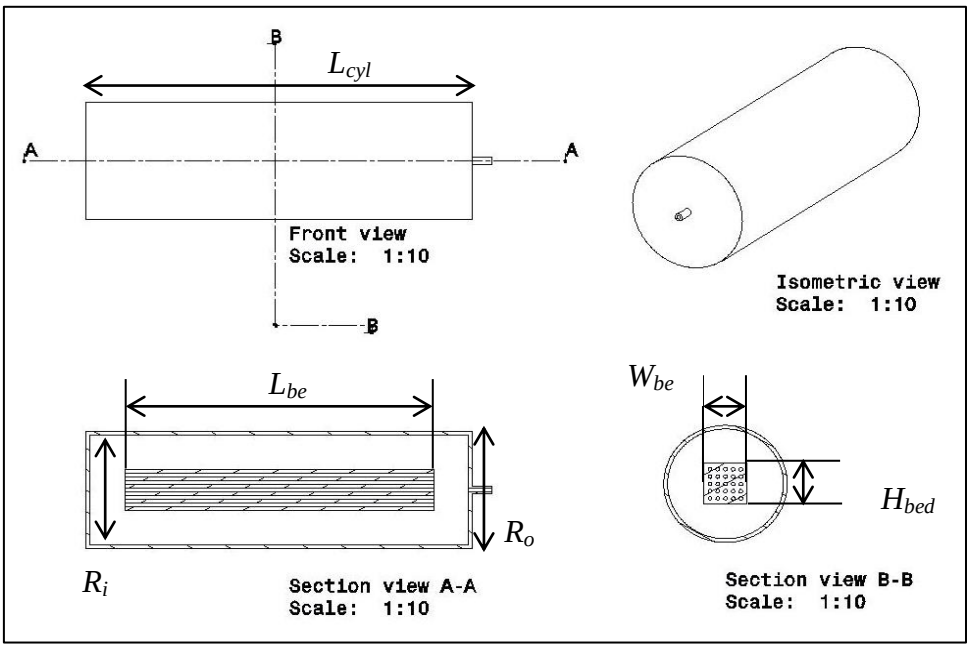

Figure 5.1.1 Benchmark design

The design for the models in this study has been done using CATIA V5 software. Based on Figure 5.1.1 above, the isometric view shows the full model of the design consisting of ANG cylinder tank with activated carbon reactor bed inside the tank. The specifications of the design can be referred to Table 5.1 below.

Table 5.1 Physical Dimension of ANG Storage Tank Assembly

Cylinder Tank			Activated Carbon Bed		
Length [m]	L_{cyl}	1.0	Length [m]	L_{bed}	0.8
Inner radius [m]	R_i	0.15	Width [m]	W_{bed}	0.112
Outer radius [m]	R_o	0.16	Height [m]	H_{bed}	0.112

For this study, the dimension of ANG cylinder tank has been fixed with the benchmark model as the author not intended to study about the characteristic of the tank but will only focusing on the reactor bed of ANG storage system. The author has proposed three designs with three difference arrangements to study the temperature and pressure variations. However, as the model seem quite simple yet it need a lot of time to determine the boundary conditions and also the parameters required for the simulation part. As for this study, the author has produced simpler models to perform simulation. The benefits of using partial models are it is faster and simpler to run the simulation and also modifications and testing can be done easily to acquire better results. The differences of simplified models with actual models is that only partial of the model geometry is being tested either at the front or middle or also at the back of the model only being tested with different parameters. Figure 5.2 below showed complete ANG Storage Model C that has been develop using CATIA V5 software. The model consist of five adsorbent bed made up from activated carbon by using the concept of baffle plate that change the direction of fluid flow to reduce the velocity thus increasing time for adsorption to take place at adsorbent pore. The holes at the adsorbent plate or bed allow methane gas to flow thus increasing the total surface area for adsorption to occur.

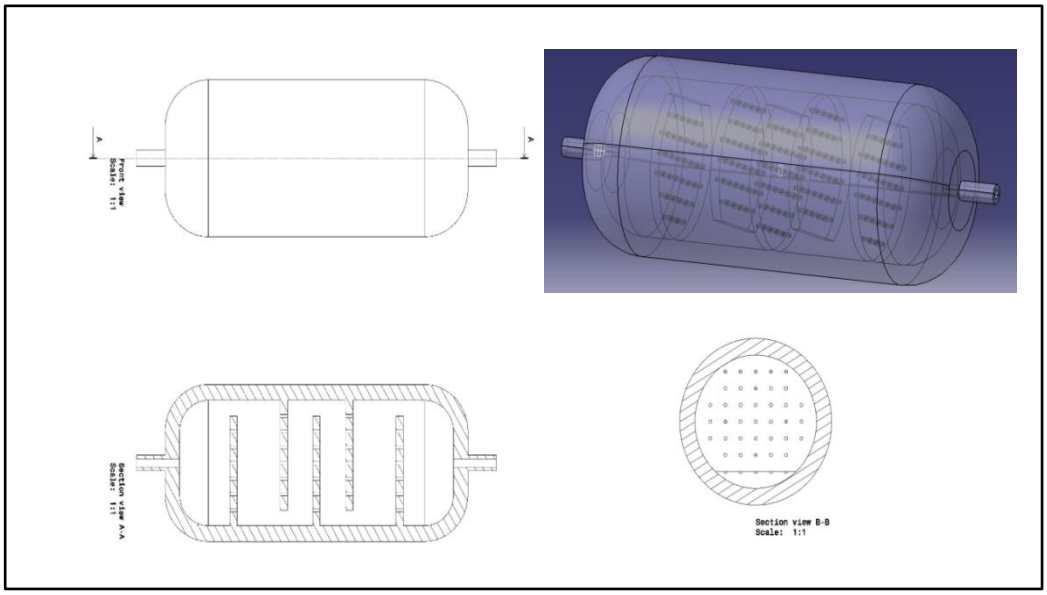

Figure 5.1.2 : ANG Storage Tank Model C

Figure 5.1.3 below showed the simplified model for ANG storage system for this study. Based on the figure, only one adsorbent bed is simulated with the operation condition that respect to overall model. For the simplified models, the reactions that occur with respect to the cylinder are neglected and focus is being directed to the reactions that occur at the reactor bed of ANG storage system.

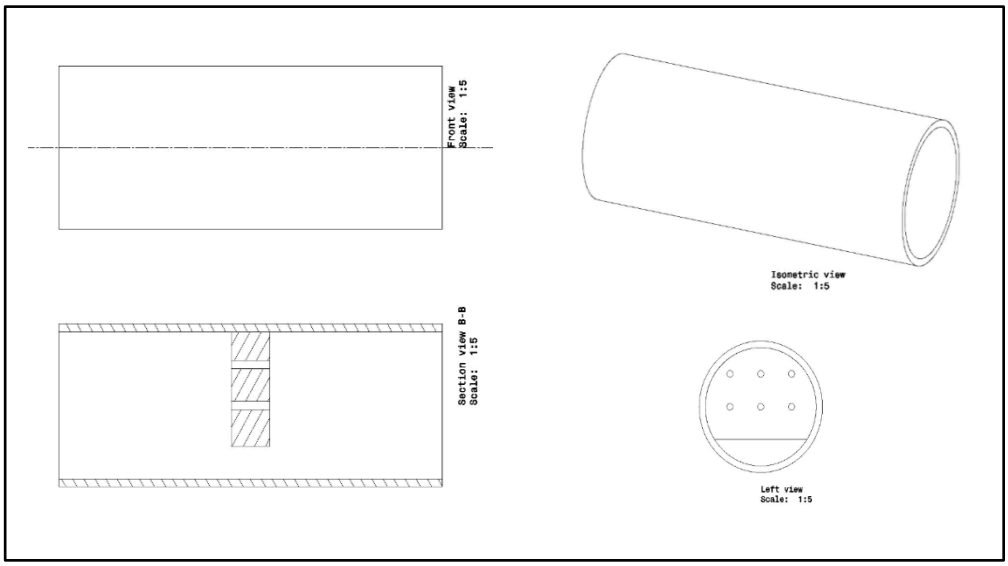

Figure 5.1.3 : Simplified Model for Pre Simulation

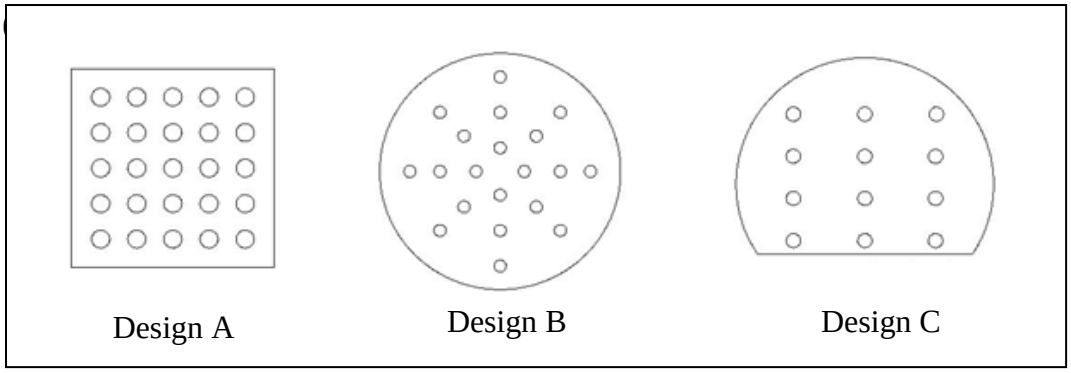

Figure 5.1.4 ANG Storage System Reactor Bed Models for Simulation

Figure 5.1.4 above showed the ANG storage system reactor bed models for simulation in this study. Based on the figure, there are three different type of design that are proposed; Design A, Design B and Design C.

5.1.1 Activated Carbon Reactor Bed Design A

Based on Figure 5.1.5 below, the author has proposed three different models for reactor bed Design A which varied in term of the number of holes and also size of holes. These three models have the same physical dimension which has rectangular shape however the total surface area exposed to adsorption is different. Design A.1 consist of 25 small holes that allow methane gas to flow inside thus increasing the total surface area for adsorption while Design A.2 and Design A.3 both consist of 9 small holes. However each design has different holes diameter. The author want to investigate the changes that will occur based on these variations.

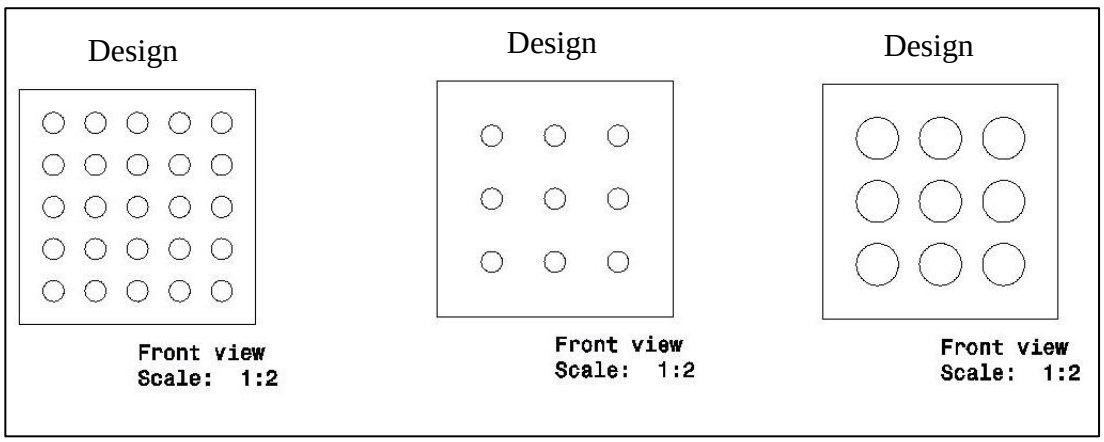

Figure 5.1.5 Reactor Design A

5.1.2 Activated Carbon Reactor Bed Design B

Based on Figure 5.1.6 below, for reactor bed Design B the author also proposed three different models which varied in term of the number of holes and also size of holes. These three models have the same physical dimension which has cylindrical shape for however the total surface area exposed to adsorption is different. Design B.1 consist of 20 small holes that allow methane gas to flow inside thus increasing the total surface area for adsorption while Design B.2 and Design B.3 both consist of 16 small holes. However each design has different holes diameter. For these models the author want to investigate the changes that will occur at the reactor bed based on these variations and compared with other designs.

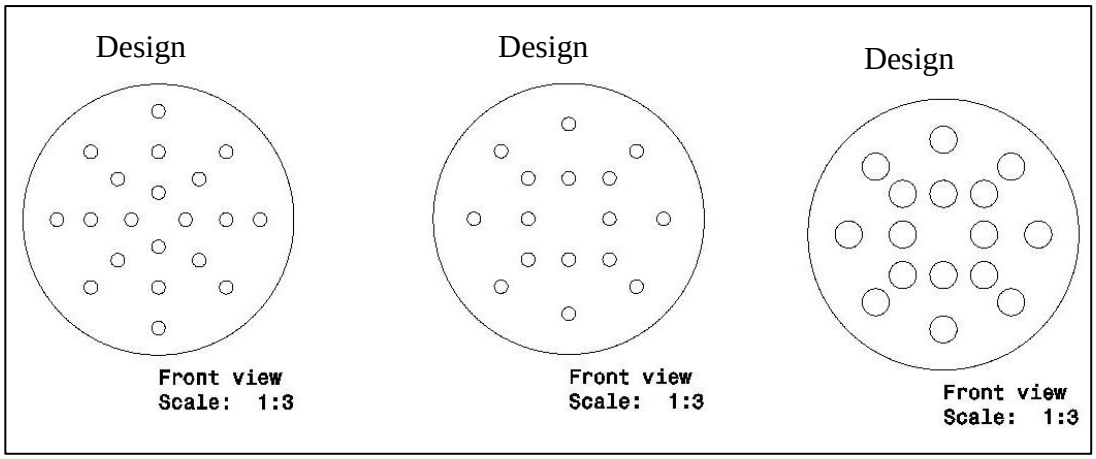

Figure 5.1.6 Reactor Design B

5.1.3 Activated Carbon Reactor Bed Design C

Based on Figure 5.1.7 below, for reactor bed Design C the author also proposed three different designs which varied in term of the number of holes and also size of holes. The model consist of five adsorbent bed made up from activated carbon by using the concept of baffle plate that change the direction of fluid flow to reduce the velocity thus increasing time for adsorption to take place at adsorbent pore. Design C.1 consist of 12 small holes that allow methane gas to flow inside thus increasing the total surface area for adsorption while Design C.2 and Design C.3 both consist of 6 small holes. However each design has different holes diameter. For these models the author want to investigate the changes that will occur at the reactor bed based on these variations and compared with other designs.

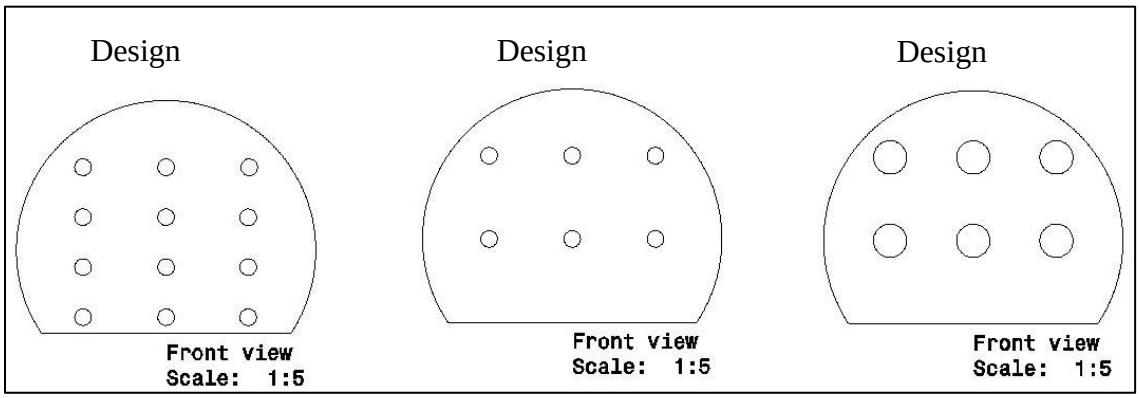

Figure 5.1.7 Reactor Design C

5.2 Simulation Setup

In order to do the simulations, the most important part is to setup all required conditions and provided enough information to the models created. For this part, the author has divided into three categories which are general conditions, cell zone conditions and boundary conditions. The most crucial part is assigning the boundary conditions since the results will depends on the information that being given. The data and information was gathered from the previous studies about ANG storage system by several scholars.

5.2.1 General Conditions

The first thing to do before doing simulation is to set the general conditions that is related to the models proposed. It is important to ensure that detail information will be provided for the simulation to run smoothly and able to give desired outcomes. Simulation basically relies on the information provided to define the conditions of the models and the environment that need to be simulated. For this study, the overall condition for the simulation is selected as pressure based condition rather than using density based since the model will be simulate based on closed container. The general model selected for this study is using energy model since this simulation will

be involve with temperature changes and heat transfer from the adsorbent to adsorbate.

At this stage, the material selection must be done together with its properties also need to be defined for all fluids and solids that will be simulated. For this study, methane, carbon and steel are selected from the FLUENT Database but the properties will be change based on the actual elements properties that are acquired from literature and can be referred to Table 5.2 below.

Table 5.2 Materials Properties

Material	Properties	Value
Methane	*Density [kg/m^3]*	0.6679
	Thermal conductivity [w/m-K]	0.0332
	Viscosity [kg/m-s]	1.087e^{-5}
	Convection coefficient [W/m^2.K]	10
Carbon (Maxsorb III)	*Specific heat capacity solid adsorbent [kJ/kg.K]*	1.375
	Conductivity of solid adsorbent [W/m.K]	0.243
	Convection coefficient solid adsorbent [W/m^2.K]	163
	Solid density [kg/m^3]	2200
	Total porosity	0.91
Steel	*Density [kg/m^3]*	8030
	Specific heat [J/kg.K]	502.48
	Thermal conductivity [w/m-K]	16.27

5.2.2 Cell Zone Conditions

After setting up general conditions for the model, the next step is to set up the cell zone conditions for either solid or fluid present inside the model. Basically, cell zones are used to assign which fluid or solid materials exist in a region. For example there are options for porous media, laminar region, fixed value and others. For this study, there are three cell zones that need to be declared which are methane, ANG

cylinder tank and reactor bed. Thus first thing to do is to determine the conditions of three zones either in fluid state or in solid state. The author has decided that methane and reactor bed are set as fluid while ANG cylinder tank as solid even though activated carbon practically a solid but it has to be set as fluid in order to give the additional input that is not present in solid state. After that, the materials for each zones need to be declared specifically and provide additional inputs if there are any. The Table 5.3 below summarizes the cell zone conditions that have been declared.

Table 5.3 Cell Zone Conditions

Cell Zone	State	Material	Optional Inputs
Methane	Fluid	Methane (CH_4)	-
Reactor Bed	Fluid	Maxsorb III	Porous Region
ANG Cylinder Tank	Solid	Steel	-

5.2.3 Boundary Conditions

The next stage in this study is to set the boundary conditions for the proposed models. In this stage, all related boundary conditions must be declared precisely as it will affect the simulation and result produce. For this study, the proposed models have 7 boundary conditions including inlet, outlet, wall of fluid, front reactor bed, back reactor bed, wall of reactor bed and inside reactor bed. For the inlet which is selected at the front of fluid (methane), is set to be a pressure inlet condition as it is suitable for both compressible and incompressible flows. A part from that, pressure inlet boundary is treated as a loss-free transition from stagnation to inlet conditions. In order to do so, FLUENT will calculates static pressure and velocity at inlet. However, mass flux through boundary varies depending on the interior solution and specified flow direction. For pressure inlet boundary condition, there are several inputs that need to be declared such as gauge total pressure, supersonic or initial gauge pressure, inlet flow direction and total temperature. The inputs for pressure inlet condition can be summarize as Table 5.4 below.

Table 5.4 Pressure Inlet Inputs

Inputs	Value
Gauge Total Pressure	3540000Pa [3]
Supersonic / Initial Gauge Pressure	101325Pa
Inlet flow direction	X-direction
Total temperature	298K

For the outlet which is selected at the back of the fluid (methane), is set to be a pressure outlet boundary condition. The advantages of using pressure outlet are it can be used for both compressible and incompressible flows, specified pressure is ignored if flow is locally supersonic at the outlet and it can be used as a "free" boundary in an external or unconfined flow. For pressure outlet boundary condition, there are several inputs that need to be declared such as gauge pressure, total temperature, target mass flow rate and backflow direction. The inputs for pressure outlet condition can be summarize as Table 5.5 below.

Table 5.5 Pressure Outlet Inputs

Inputs	Value
Gauge Pressure	3540000Pa [3]
Total temperature	303K, 308K, 313K
Target mass flow rate	0.0005kg/s
Backflow direction	X-direction

Previously, the boundary conditions for inlet and outlet have been set. Both inlet and outlet are referred back to the fluid body. For the wall of the fluid, the condition will be different from inlet and outlet. Here, the condition used is the wall boundaries where translational or rotational velocity can be applied to the wall. For this study, practically the fluid is flow into the ANG storage tank thus it has momentum inputs. The wall is set to be a moving wall with velocity of 10 m/s and moving along the X-direction. Apart from that, it also has thermal condition that has been produce due to the adsorption kinetics and also from the movement of methane molecules. For this study, it has been assigned that the fluid will carry the heat flux of 10 W/m^2 that will

transfer to the reactor bed. For the boundary conditions at front reactor bed, back reactor bed, wall of reactor bed and inside reactor bed, it has been set to be wall boundaries as well. Since all these conditions relate directly with the reactor bed, there are few similarities in term of assigning the inputs. However, the inputs values are different in due to location of the boundary. For the front reactor bed, it has been set to be a stationary wall condition with initial temperature is fixed at 298K. The material selection is set to be activated carbon thus it will has the porosity properties. On top of that, the thermal conditions also being assigned as convection with the value of 163 $W/m^2.K$ and heat of adsorption of 900 kJ/kg. For the back reactor bed, it has been set to be a stationary wall condition with temperature is varied at 303K, 308K and 313K. The material selection is set to be activated carbon thus it will has the porosity properties. On top of that, the thermal conditions also being assigned as convection with the values of 163 $W/m^2.K$ and heat of adsorption of 900 kJ/kg. Apart from that, for the wall reactor bed, it has been set to be a stationary wall condition with temperature is varied at 303K, 308K and 313K. The material selection is set to be activated carbon thus it will has the porosity properties. On top of that, the thermal conditions also being assigned as convection with the value of 163 $W/m^2.K$ and heat of adsorption of 900 kJ/kg. Last but not least, for the inside reactor bed, it has been set to be a stationary wall condition with temperature is varied at 303K, 308K and 313K. The material selection is set to be activated carbon thus it will has the porosity properties. On top of that, the thermal conditions also being assigned as convection with the value of 163 $W/m^2.K$ and heat of adsorption of 900 kJ/kg.

5.3 Simulation Results and Findings

Hundreds simulation have been conducted for the all models that have been developed throughout thus study. Since there is no previous studies have been conducted for the CFD simulation on ANG storage system, the author faced difficulties to validate the results. However, by using some of the data from the present literature especially from Rahman (2011) and also from Saha (2007), the author has generated the simulations for the reactor bed of ANG storage system. In addition, the author also produce three models with three different design to varied the results and provide more understanding toward the conditions of reactor bed for ANG storage system. The simulation aimed to see the temperature distribution and also the pressure changes at selected areas. The overall simulation for the design consisting of tank and fluid flow been made. The results of the simulation had been obtained and will be discussed.

5.3.1 Temperature Distributions

For the simulation of reactor bed of ANG storage system, the total of 27 results have been acquired for temperature distributions by using 3 designs of reactor beds with another 3 sub-designs for each making all together of 9 designs that have been involve with this study. In order to analyse the results acquired, the author have decided to focus on three main area which is the back, inside and wall of the reactor bed. The author do not want to assess the front of the reactor bed since the initial value is being fixed thus not significant changes can be seen at the area.

For the Design A at temperature 303K, it has been seen that for temperature distribution at the back reactor bed of Design A1 has the highest colour while Design A3 has the lowest colour based on contour scale. These can be referred to Figure 5.3.1.1 and Figure 5.3.1.7. On the other hand, at 303K Design A1 show the highest adsorption rate based on the highest colour produce. Basically, the higher the colour present shows more heat present at the selected area. This heat came from heat of adsorption that is being released when adsorption take place. At the wall of the reactor bed, it is seen that Design A1 also have the highest colour while Design A2 has the lowest colour based on the contour scale. The temperature variations can be

seen based on Figure 5.3.1.1 and Figure 5.3.1.4. At the area inside of the reactor or in the hole, it have been seen that Design A1 has the highest colour while Design A2 has the lowest colour based on the contour scale based on Figure 5.3.1.1 and Figure 5.3.1.4. For the analysis of Design A at temperature 308K, the temperature distributions at the back of the reactor bed shows that Design A1 has the highest colour and Design A3 has the lowest colour based on the contour scale based on Figure 5.3.1.2 and Figure 5.3.1.8. Looking at the wall of the reactor bed, it have been seen that Design A3 has the highest colour and Design A2 has the lowest colour changes based on Figure 5.3.1.8 and Figure 5.3.1.5. At the inside of the reactor bed shows that the temperature changes are the same as the changes happen at the wall of reactor bed. For the analysis at temperature 313K, it has been seen that at the back of the reactor bed shows that Design A1 has the highest colour while Design A3 has the lowest based on the contour scale and can be referred to Figure 5.3.1.3 and Figure 5.3.1.9. At the wall of the reactor bed, it has been seen that, Design A3 has the highest colour while Design A2 has the lowest colour changes based on Figure 5.3.1.9 and Figure 5.3.1.6. It also been seen that the temperature changes inside of the reactor bed followed the changes occur at the wall of the reactor bed.

For the Design B at temperature 303K, it has been seen that for temperature distribution at the back reactor bed of Design B3 has the highest colour while Design B1 has the lowest colour based on contour scale and can be seen from Figure 5.3.1.16 and Figure 5.3.1.10. At the wall of the reactor bed, it is seen that Design B3 also have the highest colour while Design B2 has the lowest colour based on the contour scale. These can be referred to Figure 5.3.1.16 and Figure 5.3.1.13. At the area inside of the reactor or in the hole, it have been seen that Design B3 has the highest colour while Design B1 has the lowest colour based on the contour scale and can be referred to Figure 5.3.1.16 and Figure 5.3.1.10. For the analysis of Design B at temperature 308K, the temperature distributions at the back of the reactor bed shows that Design B3 has the highest colour and Design B1 has the lowest colour based on the contour scale and can be referred to Figure 5.3.1.17 and Figure 5.3.1.11. Looking at the wall of the reactor bed, it have been seen that Design B3 has the highest colour and Design B2 has the lowest colour changes from Figure 5.3.1.17 and Figure 5.3.1.14. At the inside of the reactor bed shows that the temperature changes are the same as the changes happen at the wall of reactor bed. For the

analysis at temperature 313K, it has been seen that at the back of the reactor bed shows that Design B3 has the highest colour while Design B2 has the lowest based on the contour scale. The temperature variations can both be referred to Figure 5.3.1.18 and Figure 5.3.1.15. At the wall of the reactor bed, it has been seen that, Design B3 has the highest colour while Design B2 has the lowest colour changes based on Figure 5.3.1.18 and Figure 5.3.1.15. It also been seen that the temperature changes inside of the reactor bed followed the changes occur at the wall of the reactor bed.

For the Design C at temperature 303K, it has been seen that for temperature distribution at the back reactor bed of Design C1 has the highest colour while Design C2 has the lowest colour based on contour scale. At the wall of the reactor bed, it is seen that Design C1 also have the highest colour while Design C2 has the lowest colour based on the contour scale. At the area inside of the reactor or in the hole, it have been seen that Design C1 has the highest colour while Design C2 has the lowest colour based on the contour scale. For the analysis at temperature 303K can be referred to Figure 5.3.1.19 and Figure 5.3.1.22. For the analysis of Design C at temperature 308K, the temperature distributions at the back of the reactor bed shows that Design C2 has the highest colour and Design C3 has the lowest colour based on the contour scale. Looking at the wall of the reactor bed, it have been seen that Design C2 has the highest colour and Design C3 has the lowest colour changes. At the inside of the reactor bed shows that the temperature changes are the same as the changes happen at the wall of reactor bed. . For the analysis at temperature 308K can be referred to Figure 5.3.1.23 and Figure 5.3.1.26. For the analysis at temperature 313K, it has been seen that at the back of the reactor bed shows that Design C1 has the highest colour while Design C3 has the lowest based on the contour scale from Figure 5.3.1.21 and Figure 5.3.1.27. At the wall of the reactor bed, it has been seen that, Design C2 has the highest colour while Design C3 has the lowest colour changes. It also been seen that the temperature changes inside of the reactor bed followed the changes occur at the wall of the reactor bed. These can be referred to Figure 5.3.1.24 and Figure 5.3.1.27. The complete results of simulation for temperature distribution at the reactor bed of ANG storage system can be seen from the figures below.

Design A.1

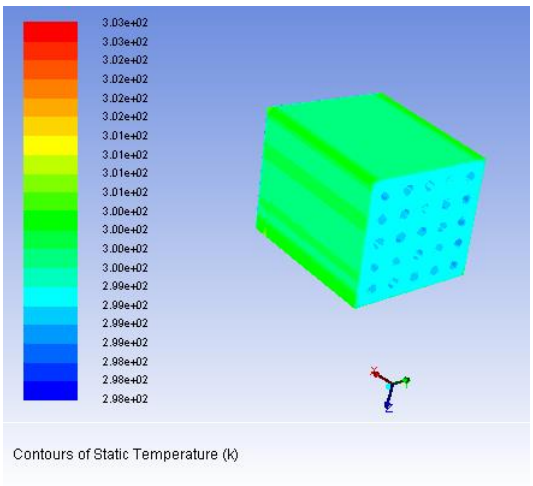

Figure 5.3.1.1 Design A1 ANG Reactor Bed at Temperature 303K

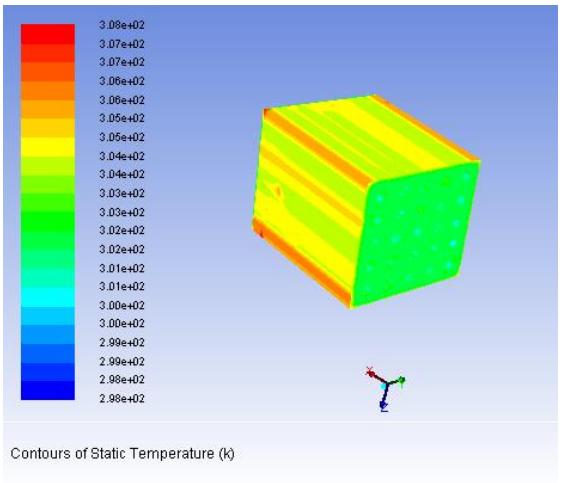

Figure 5.3.1.2 Design A1 ANG Reactor Bed at Temperature 308K

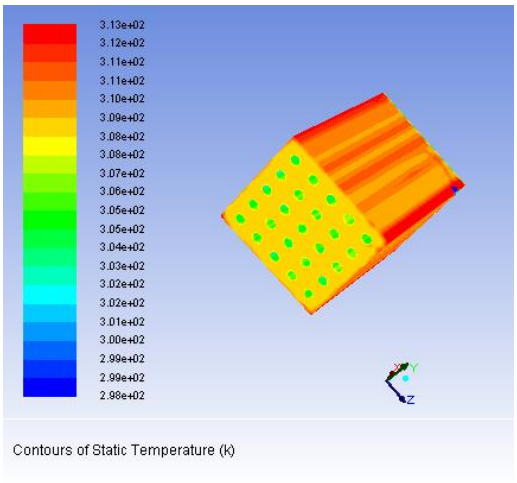

Figure 5.3.1.3 Design A1 ANG Reactor Bed at Temperature 313K

Design A.2

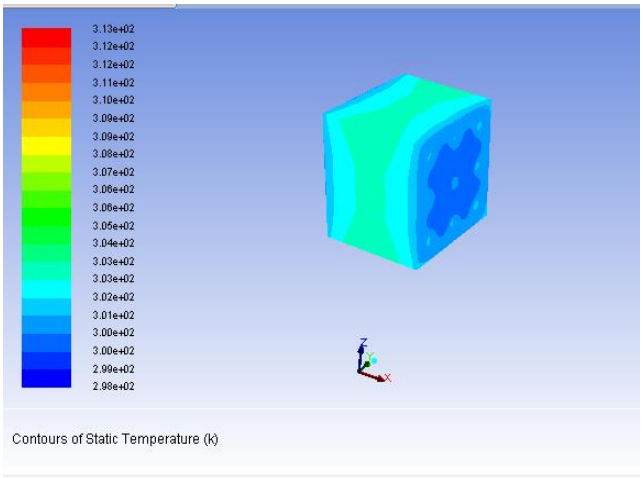

Figure 5.3.1.4 Design A2 ANG Reactor Bed at Temperature 303K

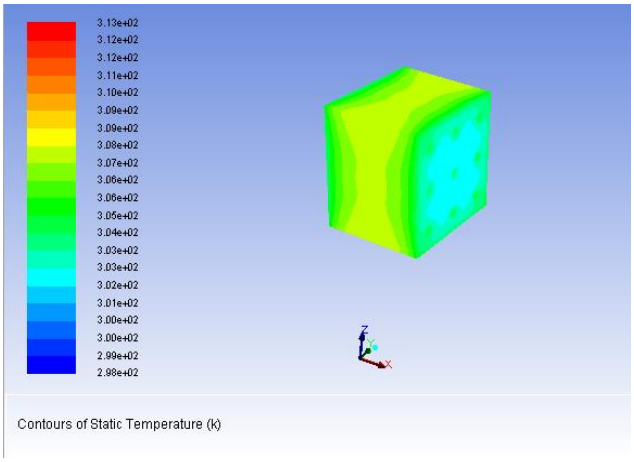

Figure 5.3.1.5 Design A2 ANG Reactor Bed at Temperature 308K

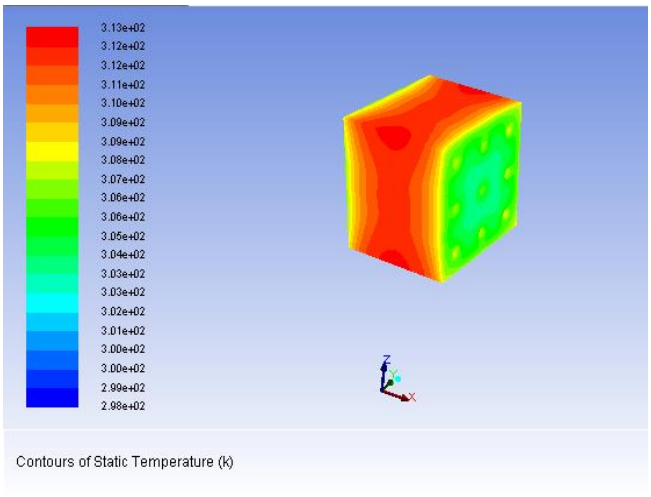

Figure 5.3.1.6 Design A2 ANG Reactor Bed at Temperature 313K

Design A.3

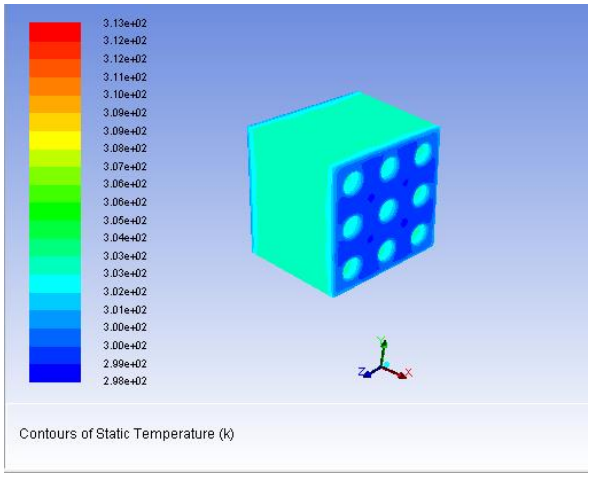

Figure 5.3.1.7 Design A3 ANG Reactor Bed at Temperature 303K

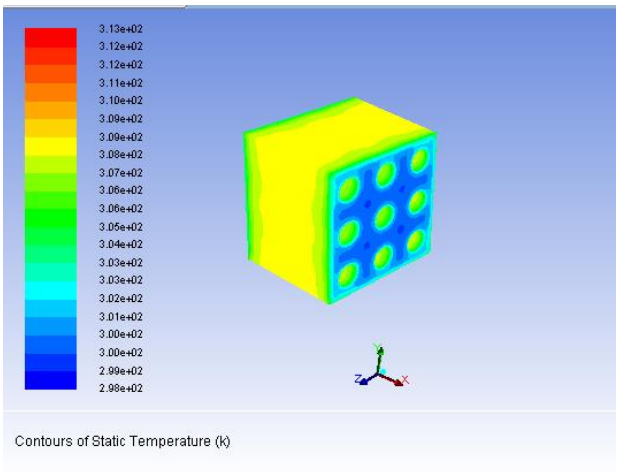

Figure 5.3.1.8 Design A3 ANG Reactor Bed at Temperature 308K

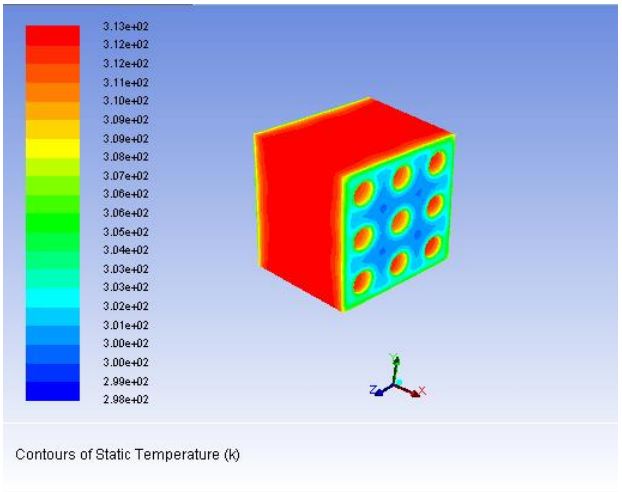

Figure 5.3.1.9 Design A3 ANG Reactor Bed at Temperature 313K

Design B.1

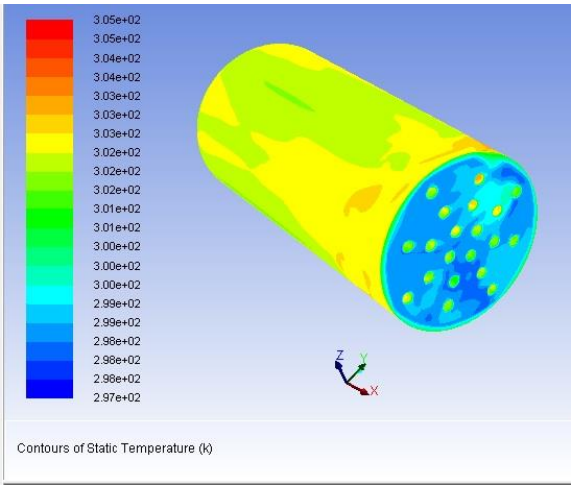

Figure 5.3.1.10 Design B1 ANG Reactor Bed at Temperature 303K

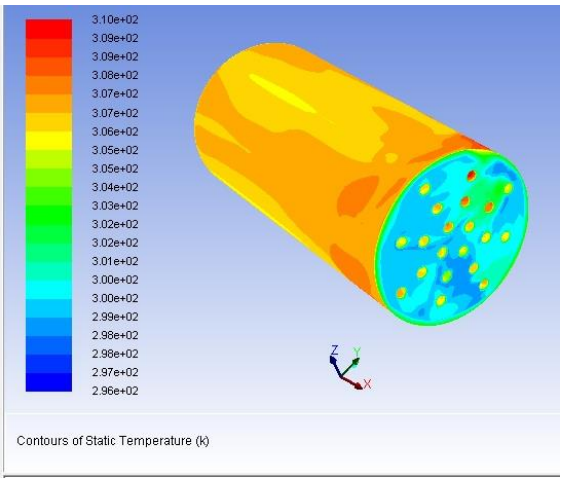

Figure 5.3.1.11 Design B1 ANG Reactor Bed at Temperature 308K

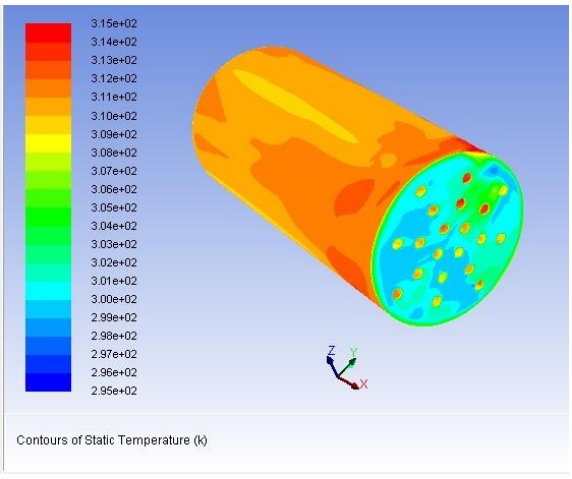

Figure 5.3.1.12 Design B1 ANG Reactor Bed at Temperature 313K

Design B.2

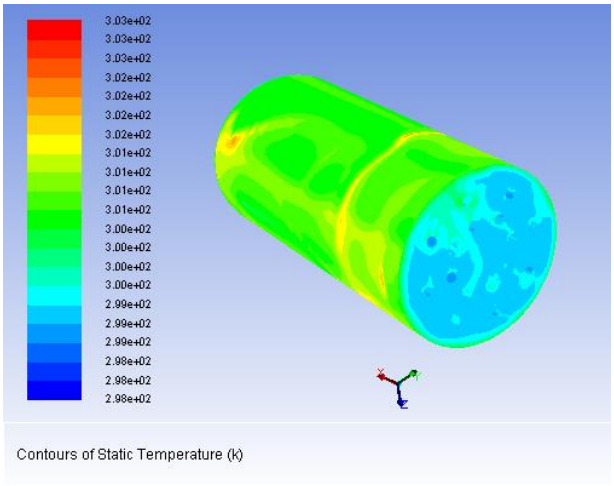

Figure 5.3.1.13 Design B2 ANG Reactor Bed at Temperature 303K

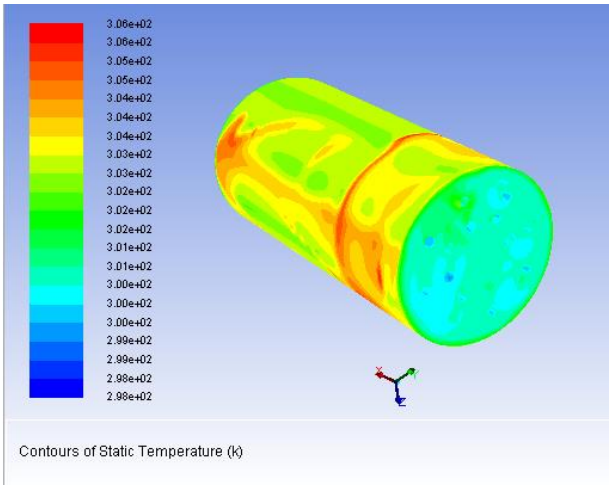

Figure 5.3.1.14 Design B2 ANG Reactor Bed at Temperature 308K

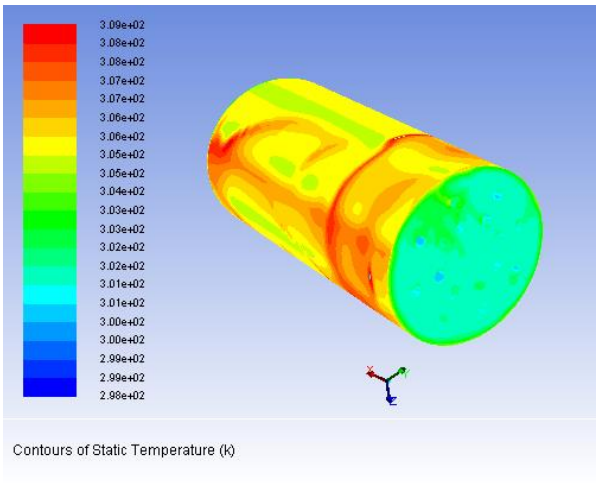

Figure 5.3.1.15 Design B2 ANG Reactor Bed at Temperature 313K

Design B.3

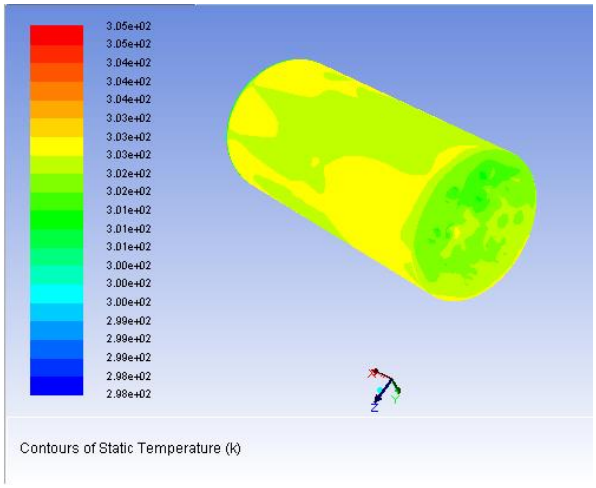

Figure 5.3.1.16 Design B3 ANG Reactor Bed at Temperature 303K

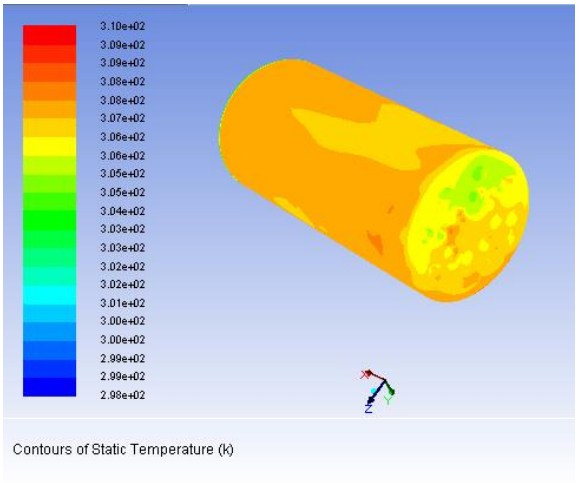

Figure 5.3.1.17 Design B3 ANG Reactor Bed at Temperature 308K

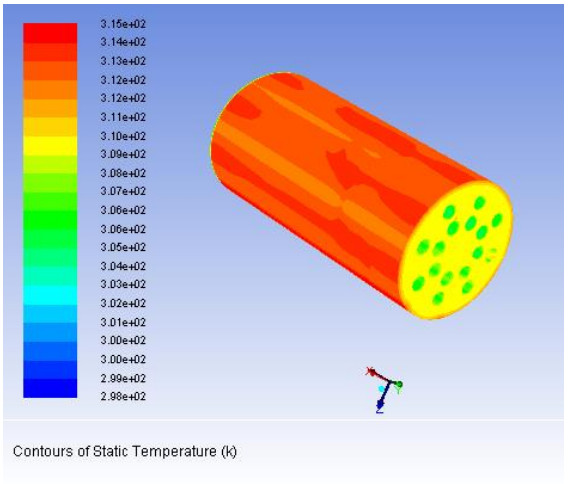

Figure 5.3.1.18 Design B3 ANG Reactor Bed at Temperature 313K

Design C.1

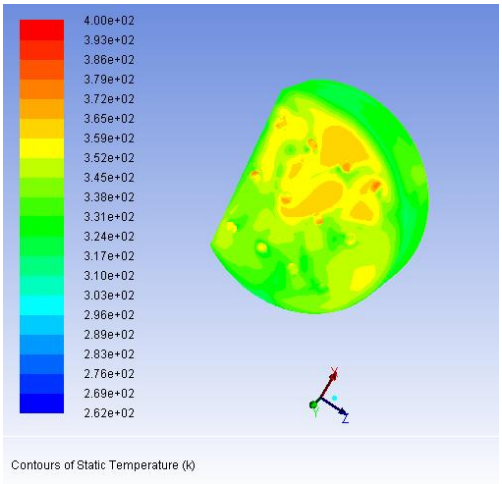

Figure 5.3.1.19 Design C1 ANG Reactor Bed at Temperature 303K

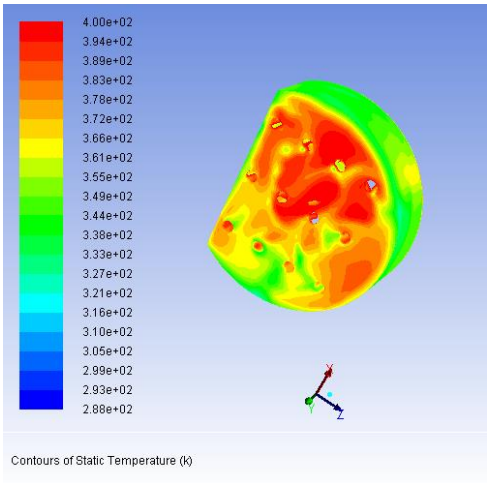

Figure 5.3.1.20 Design C1 ANG Reactor Bed at Temperature 308K

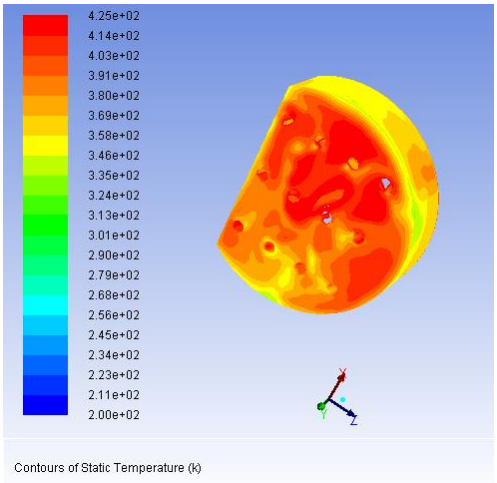

Figure 5.3.1.21 Design C1 ANG Reactor Bed at Temperature 313K

Design C.2

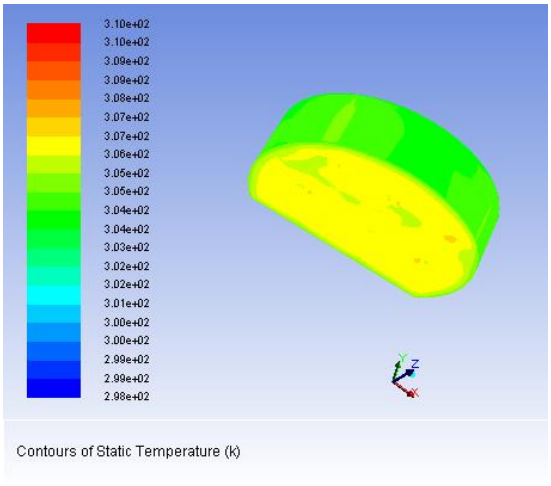

Figure 5.3.1.22 Design C2 ANG Reactor Bed at Temperature 303K

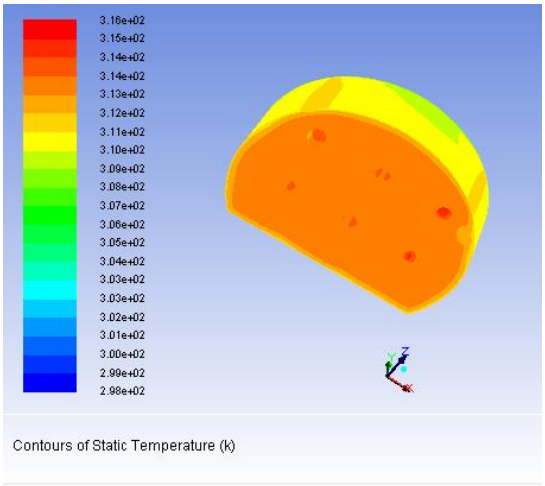

Figure 5.3.1.23 Design C2 ANG Reactor Bed at Temperature 308K

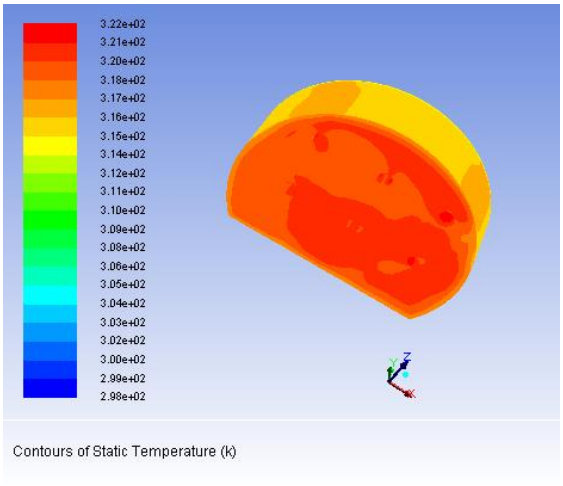

Figure 5.3.1.24 Design C2 ANG Reactor Bed at Temperature 313K

Design C.3

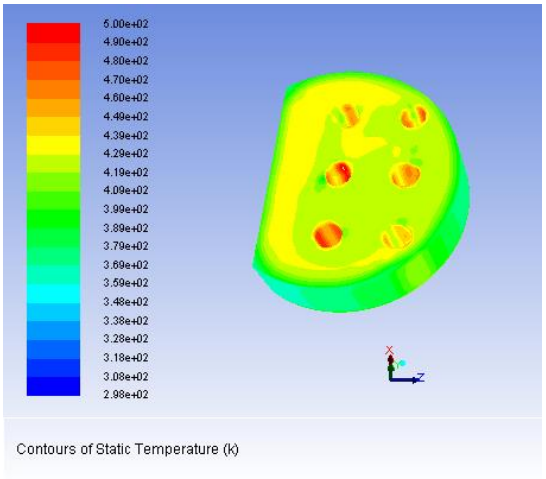

Figure 5.3.1.25 Design C3 ANG Reactor Bed at Temperature 303K

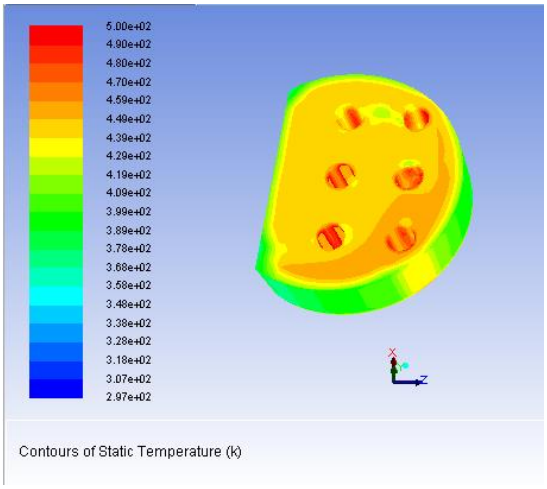

Figure 5.3.1.26 Design C3 ANG Reactor Bed at Temperature 308K

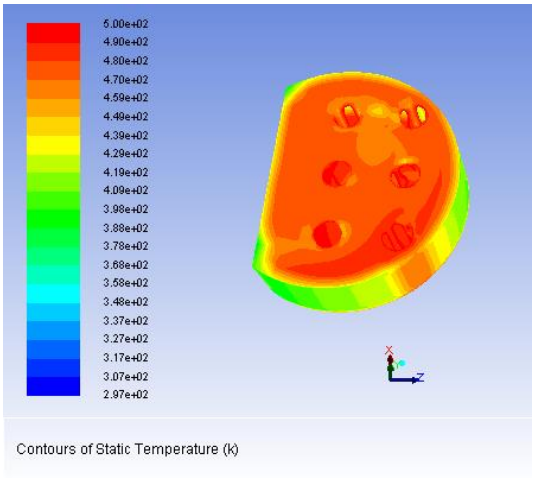

Figure 5.3.1.27 Design C3 ANG Reactor Bed at Temperature 313K

5.3.2 Pressure Distributions

For the simulation of pressure distribution for reactor bed of ANG storage system, the total of 27 results also have been acquired for temperature distributions by using 3 designs of reactor beds with another 3 sub-designs for each making all together of 9 designs that have been involve with this study. In order to analyse the results acquired, the author have decided to focus on three main area which is the back, inside and wall of the reactor bed. The author do not want to assess the front of the reactor bed since the initial value is being fixed thus not significant changes can be seen at the area. The simulations have been completed at three different temperature; 303K, 308K and 313K and the pressure distribution at the reactor bed of ANG storage system are analyses based on these three temperature.

For the Design A at temperature 303K, it has been seen that for pressure distribution at the back reactor bed of Design A2 has the highest colour while Design A3 has the lowest colour based on pressure contour scale and can be seen from Figure 5.3.2.4 and Figure 5.3.2.7. At the wall of the reactor bed, it is seen that Design A2 also have the highest colour while Design A3 has the lowest colour based on the pressure contour scale and can be seen from Figure 5.3.2.4 and Figure 5.3.2.7. At the area inside of the reactor or in the hole, it have been seen that Design A2 has the highest colour while Design A3 has the lowest colour based on the contour scale also can be seen from Figure 5.3.2.4 and Figure 5.3.2.7. For the pressure analysis of Design A at temperature 308K, the pressure distributions at the back of the reactor bed shows that Design A2 has the highest colour and Design A3 has the lowest colour based on the pressure contour scale and can be seen from Figure 5.3.2.5 and Figure 5.3.2.8. Looking at the wall of the reactor bed, it have been seen that Design A2 has the highest colour and Design A3 has the lowest colour changes. At the inside of the reactor bed shows that the pressure changes are the same as the changes happen at the wall of reactor bed and can be seen from Figure 5.3.2.5 and Figure 5.3.2.8. For the pressure analysis at temperature 313K, it has been seen that pressure distributions at the back of the reactor bed shows that Design A1 has the highest colour while Design A3 has the lowest based on the pressure contour scale and can be seen from Figure 5.3.2.3 and Figure 5.3.2.9. At the wall of the reactor bed, it has been seen that, Design A1 has the highest colour while Design A3 has the lowest

colour changes. It also been seen that the pressure changes inside of the reactor bed followed the changes occur at the wall of the reactor bed and can be seen from Figure 5.3.2.3 and Figure 5.3.2.9.

For the Design B at temperature 303K, it has been seen that for pressure distributions at the back reactor bed of Design B1 has the highest colour while Design B3 has the lowest colour based on pressure contour scale. At the wall of the reactor bed, it is seen that Design B1 also have the highest colour while Design B3 has the lowest colour based on the contour scale. At the area inside of the reactor or in the hole, it have been seen that pressure distributions at Design B1 has the highest colour while Design B3 has the lowest colour based on the contour scale. For the analysis of Design B at temperature 308K, the pressure distributions at the back of the reactor bed shows that Design B1 has the highest colour and Design B3 has the lowest colour based on the contour scale. Looking at the wall of the reactor bed, it have been seen that pressure distributions at Design B1 has the highest colour and Design B3 has the lowest colour changes. At the inside of the reactor bed shows that the pressure changes are the same as the changes happen at the wall of reactor bed. For the analysis at temperature 313K, it has been seen that at the back of the reactor bed shows that pressure distributions at Design B1 has the highest colour while Design B3 has the lowest based on the contour scale. At the wall of the reactor bed, it has been seen that, Design B1 has the highest colour while Design B3 has the lowest colour changes. It also been seen that the pressure changes inside of the reactor bed followed the changes occur at the wall of the reactor bed.

For the Design C at temperature 303K, it has been seen that for pressure distributions at the back reactor bed of Design C2 has the highest colour while Design C1 has the lowest colour based on pressure contour scale. At the wall of the reactor bed, it is seen that Design C2 also have the highest colour while Design C1 has the lowest colour based on the pressure contour scale. At the area inside of the reactor or in the hole, it have been seen that pressure distributions at Design C2 has the highest colour while Design C1 has the lowest colour based on the contour scale. For the pressure analysis of Design C at temperature 308K, the pressure distributions at the back of the reactor bed shows that Design C2 has the highest colour and Design C3 has the lowest colour based on the contour scale. Looking at the wall of

the reactor bed, it have been seen that pressure distributions at Design C1 has the highest colour and Design C3 has the lowest colour changes. At the inside of the reactor bed shows that the pressure changes are the same as the changes happen at the wall of reactor bed. For the analysis at temperature 313K, it has been seen that at the back of the reactor bed shows that pressure distributions at Design C2 has the highest colour while Design C3 has the lowest based on the pressure contour scale. At the wall of the reactor bed, it has been seen that, Design C2 has the highest colour while Design C3 has the lowest colour changes. It also been seen that the pressure changes inside of the reactor bed followed the changes occur at the wall of the reactor bed. The complete results of simulation for pressure distribution at the reactor bed of ANG storage system can be seen from the figures below.

Design A.1

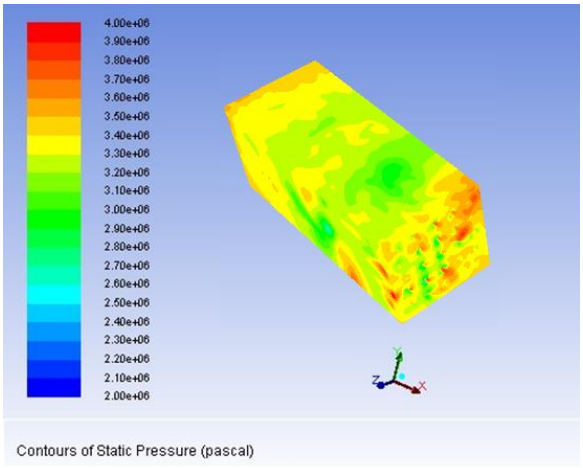

Figure 5.3.2.1 Design A1 Pressure Variation at ANG Reactor Bed at 303K

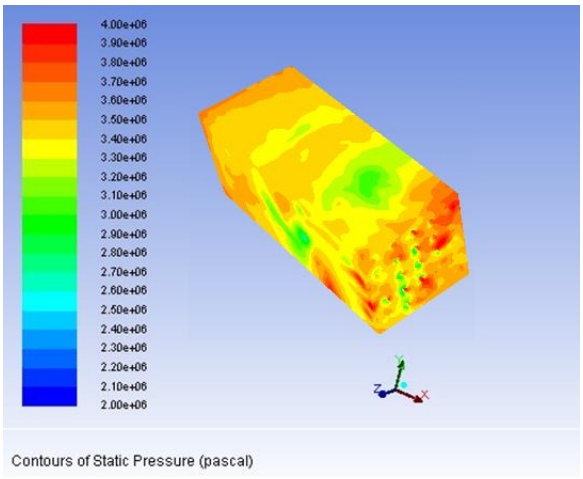

Figure 5.3.2.2 Design A1 Pressure Variation at ANG Reactor Bed at 308K

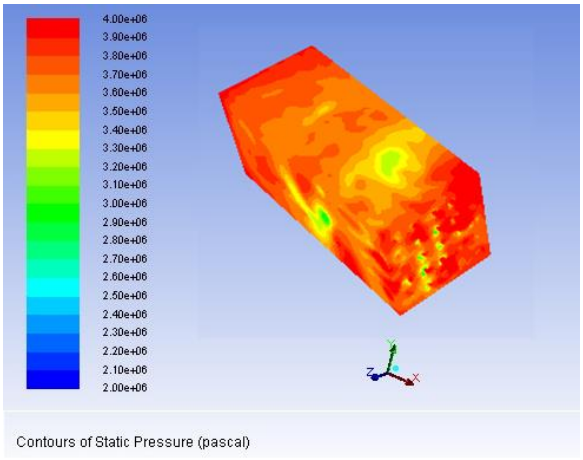

Figure 5.3.2.3 Design A1 Pressure Variation at ANG Reactor Bed at 313K

Design A.2

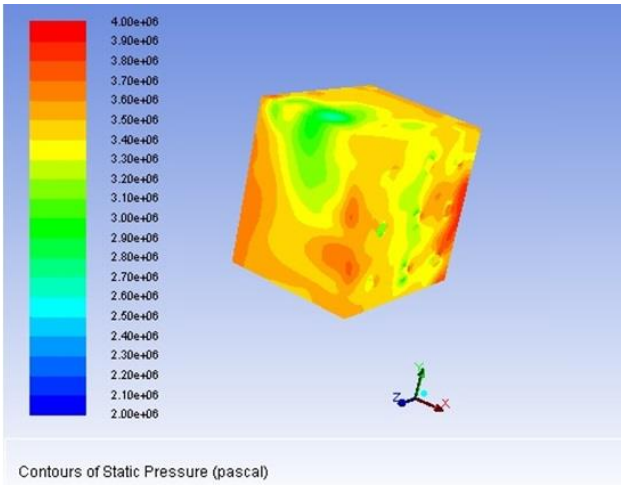

Figure 5.3.2.4 Design A2 Pressure Variation at ANG Reactor Bed at 303K

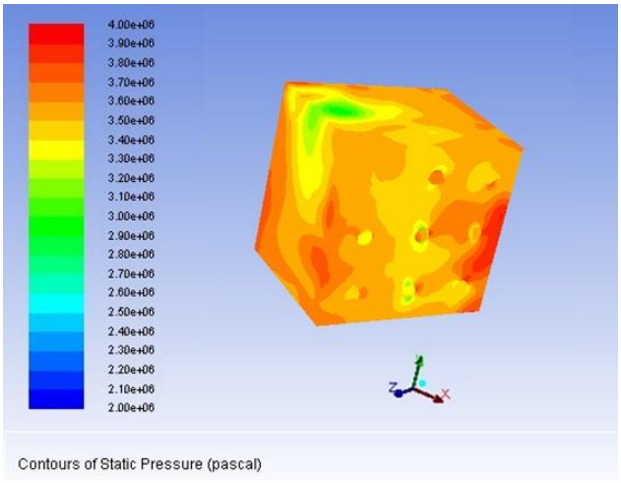

Figure 5.3.2.5 Design A2 Pressure Variation at ANG Reactor Bed at 308K

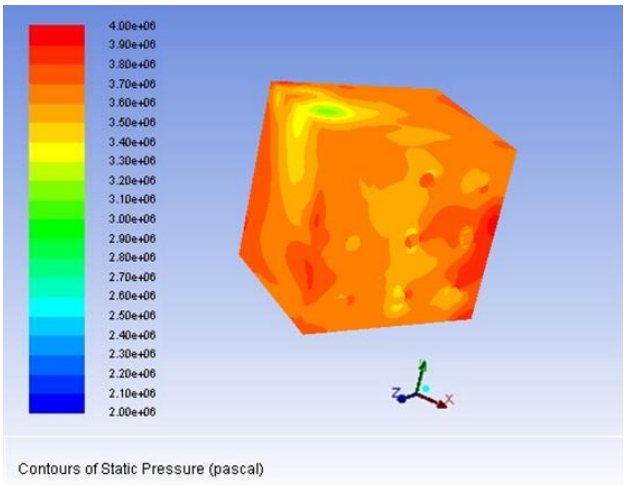

Figure 5.3.2.6 Design A2 Pressure Variation at ANG Reactor Bed at 313K

Design A.3

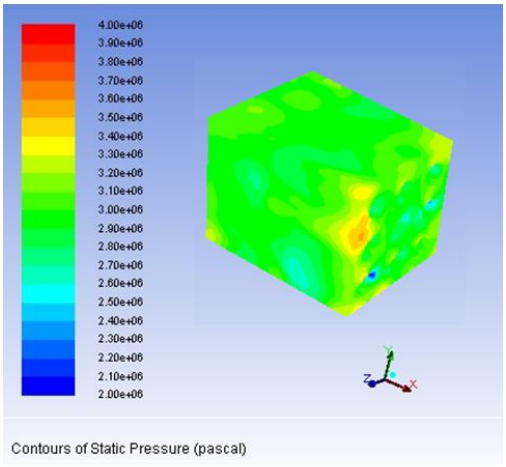

Figure 5.3.2.7 Design A3 Pressure Variation at ANG Reactor Bed at 303K

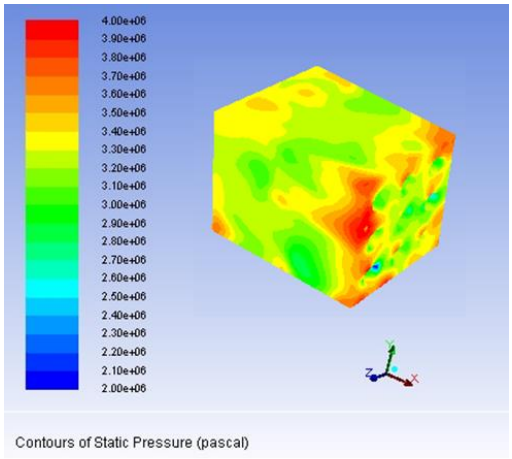

Figure 5.3.2.8 Design A3 Pressure Variation at ANG Reactor Bed at 308K

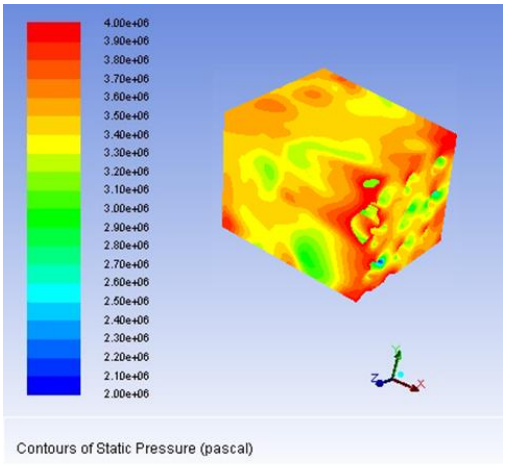

Figure 5.3.2.9 Design A3 Pressure Variation at ANG Reactor Bed at 313K

Design B.1

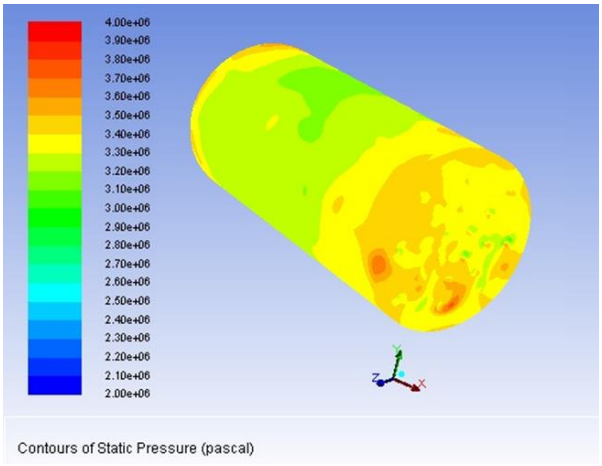

Figure 5.3.2.10 Design B1 Pressure Variation at ANG Reactor Bed at 303K

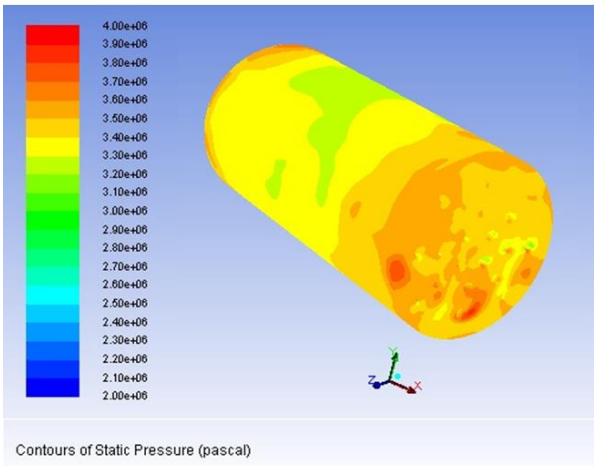

Figure 5.3.2.11 Design B1 Pressure Variation at ANG Reactor Bed at 308K

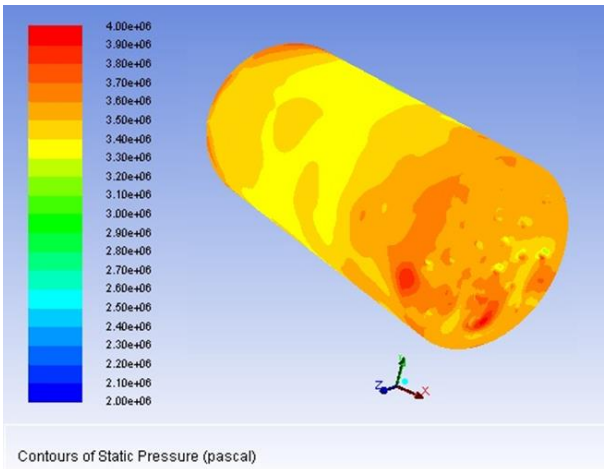

Figure 5.3.2.12 Design B1 Pressure Variation at ANG Reactor Bed at 313K

Design B.2

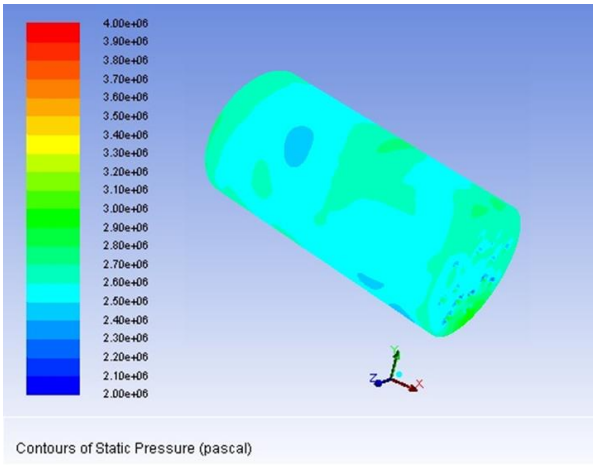

Figure 5.3.2.13 Design B2 Pressure Variation at ANG Reactor Bed at 303K

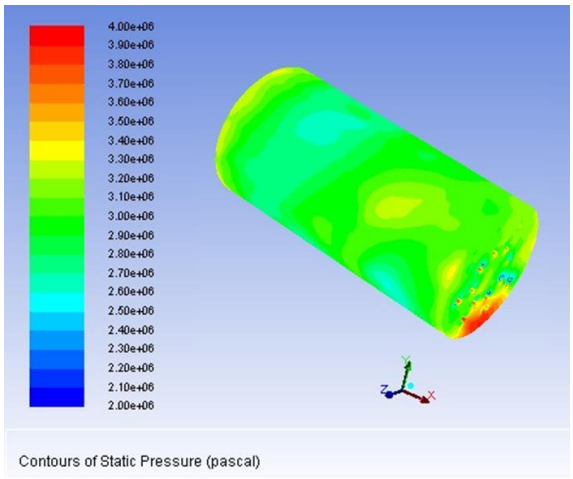

Figure 5.3.2.14 Design B2 Pressure Variation at ANG Reactor Bed at 308K

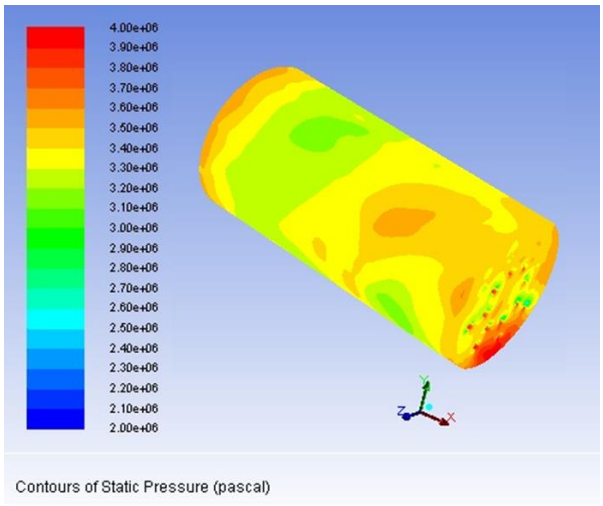

Figure 5.3.2.15 Design B2 Pressure Variation at ANG Reactor Bed at 313K

Design B.3

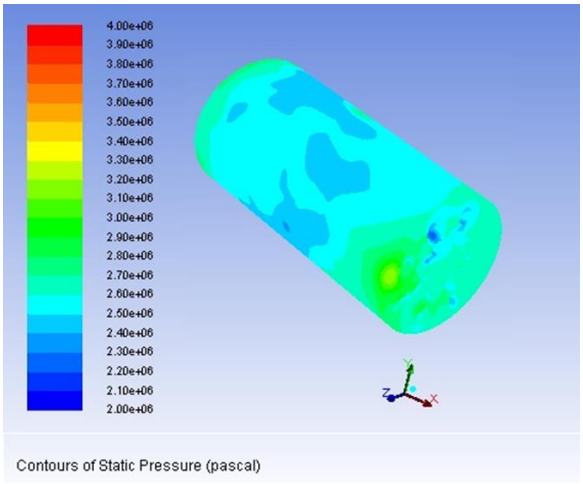

Figure 5.3.2.16 Design B3 Pressure Variation at ANG Reactor Bed at 303K

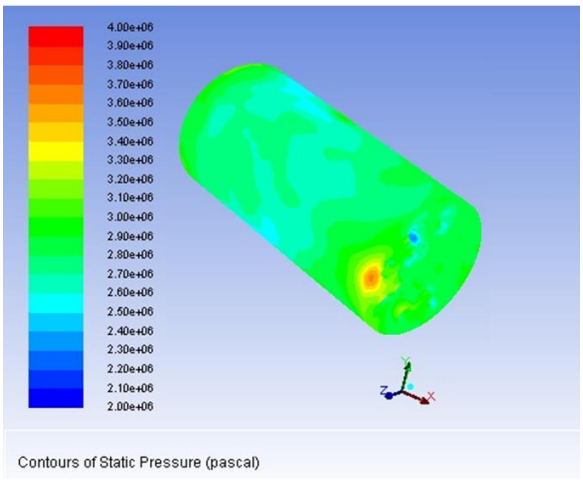

Figure 5.3.2.17 Design B3 Pressure Variation at ANG Reactor Bed at 308K

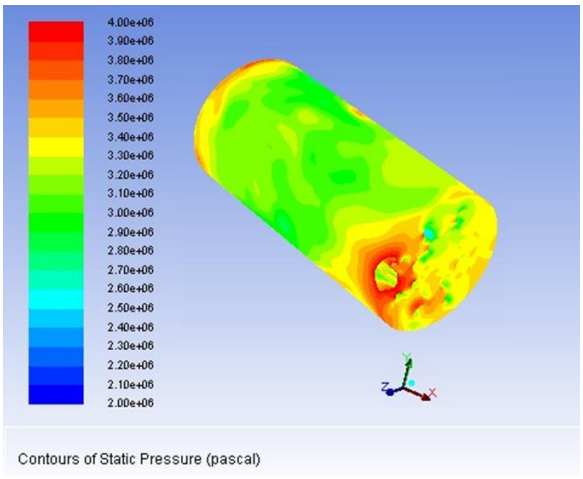

Figure 5.3.2.18 Design B3 Pressure Variation at ANG Reactor Bed at 313K

Design C.1

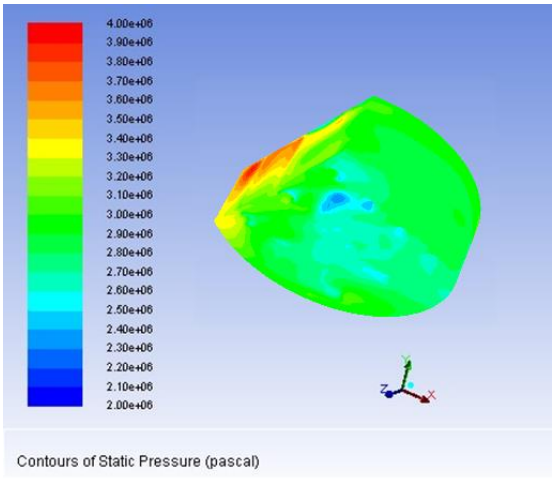

Figure 5.3.2.19 Design C1 Pressure Variation at ANG Reactor Bed at 303K

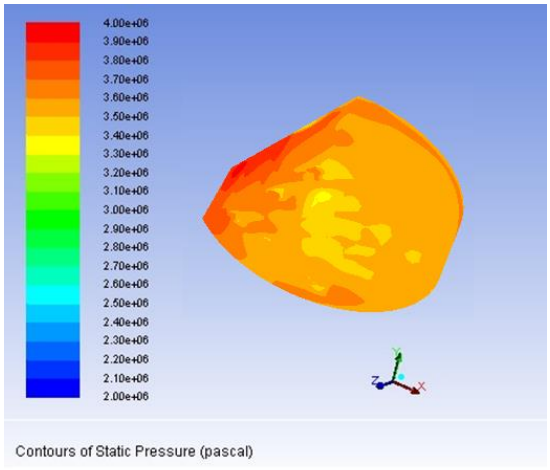

Figure 5.3.2.20 Design C1 Pressure Variation at ANG Reactor Bed at 308K

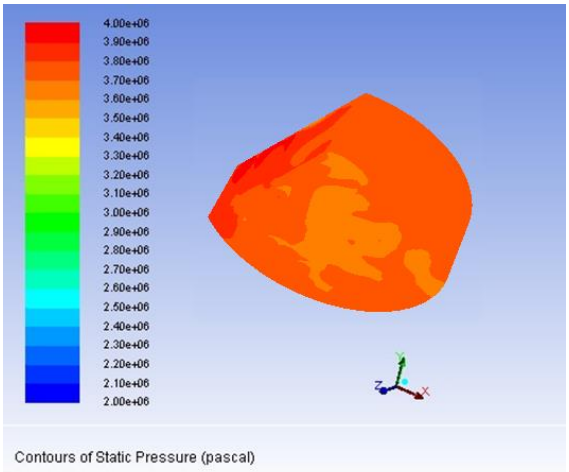

Figure 5.3.2.21 Design C1 Pressure Variation at ANG Reactor Bed at 313K

Design C.2

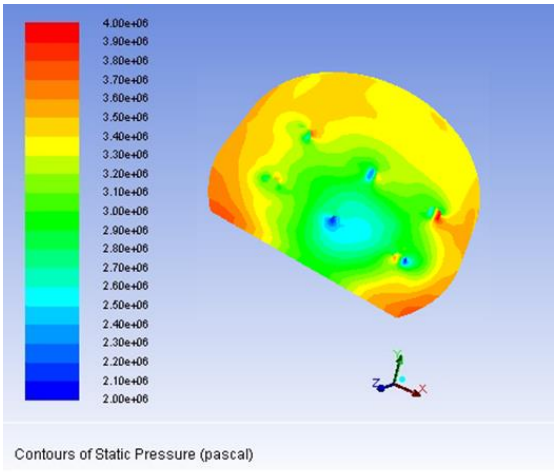

Figure 5.3.2.22 Design C2 Pressure Variation at ANG Reactor Bed at 303K

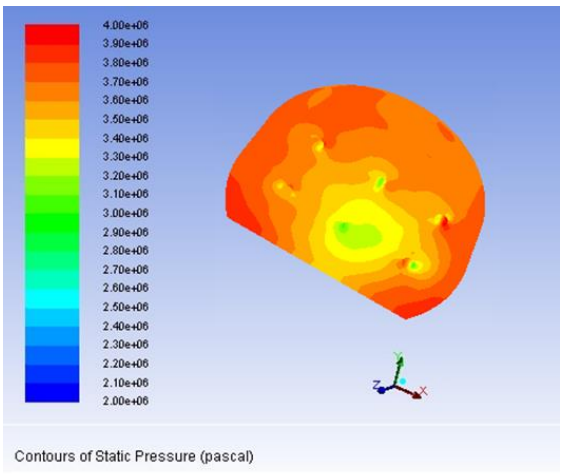

Figure 5.3.2.23 Design C2 Pressure Variation at ANG Reactor Bed at 308K

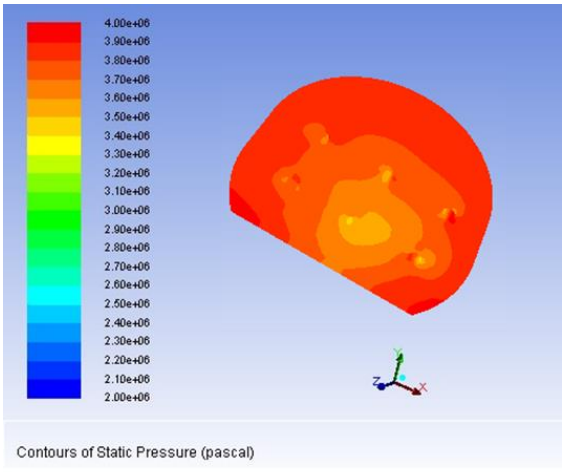

Figure 5.3.2.24 Design C2 Pressure Variation at ANG Reactor Bed at 313K

Design C.3

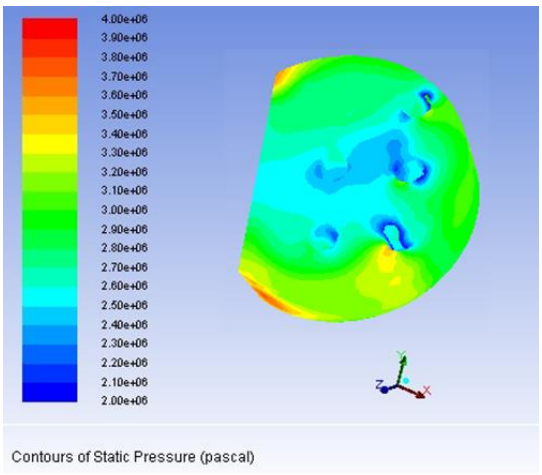

Figure 5.3.2.25 Design C3 Pressure Variation at ANG Reactor Bed at 303K

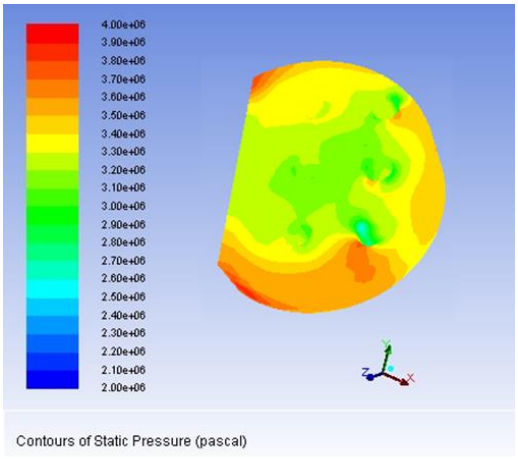

Figure 5.3.2.26 Design C3 Pressure Variation at ANG Reactor Bed at 308K

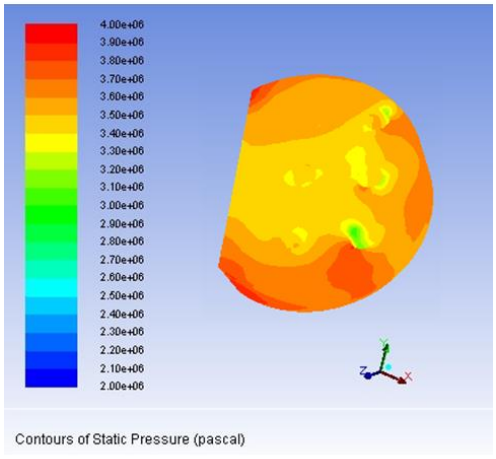

Figure 5.3.2.27 Design C3 Pressure Variation at ANG Reactor Bed at 313K

5.4 Discussion and Analysis

Based on the objectives of this study which consist of two main concerned which are to study the effect of different designs for ANG storage reactor bed system toward the adsorption of methane gas and to analyze the pressure and temperature distributions at the reactor bed of ANG storage system due to the adsorption of methane gas. Referring back to Figure 5.1.4, this study has proposed 3 different designs with another 3 sub-designs for each. The purposed of producing these designs is to relate back with the first objective of this study itself and most important thing is that its relate with the second objective of this study which is to analyse the pressure and temperature variation at reactor bed of ANG storage system.

Based on the results of temperature distributions, it has been found that at temperature 303K the temperature contour begin to spread around the front, back, wall and inside of the reactor beds. At this stage, the molecules of methane start to filling up the pores of the activated carbon at the reactor bed and releasing small amount of heat of adsorption. The contour of reactor bed can be seen with blue to the green colour indicating low temperature changes occur. As the process going to temperature 308K, more methane molecules being adsorbed by the activated carbon releasing large amount of heat and the contour colour of reactor bed change into yellowish to orange colour and this can be seen clearly at temperature 313K as the reactor bed turn into red contour indicating the highest temperature changes occur at the reactor bed. As for Design A, temperature distributions results show that Design A3 has the highest contour changes and while Design A2 has the lowest changes. Based on three sub-design for Design A, Design A3 has the highest total surface area exposed to the methane gas flow inside the ANG tank compare to Design A2 and A1. On the other hand, Design A2 has the lowest total surface area exposed to the methane gas flow inside the tank. As for Design B, it has found that the temperature distributions at reactor bed of Design B3 has the highest contour changes and while Design B2 has the lowest changes. Based on three sub-design for Design B, Design B3 has the highest total surface area exposed to the methane gas flow inside the ANG tank compare to Design B2 and B1. On the other hand, Design B2 has the lowest total surface area exposed to the methane gas flow inside the tank. As for

Design C, temperature distributions results show that Design C1 has the highest contour changes and while Design C3 has the lowest changes. Based on three sub-designs for Design C, Design C3 has the highest total surface area exposed to the methane gas flow inside the ANG tank compare to Design C2 and C1. On the other hand, Design C2 has the lowest total surface area exposed to the methane gas flow inside the tank. However, the results achieved for Design C is little bit different from Design A and B, this is due to the total volume of reactor bed effect the changes that occur to Design C. Basically Design C used the concept of baffle plate separation as in separator to reduce the velocity of the fluid thus more adsorption time can be provided to the reactor bed. However, the total volume of reactor is minimum as it need to be separate into small compartment compared to Design A and B that have bulky reactor bed. Based on these situations, it has been found that as the temperature of the bed increases the distribution of temperature contour also increase. However, for ANG storage system to perform efficiently, the temperature must be kept at lower temperature since the adsorption rate decrease with increase of temperature.

Based on the results of pressure distributions, it has been found that at temperature 303K the pressure contour begin to spread around the front, back, wall and inside of the reactor beds. At this stage, the molecules of methane start to filling up the pores of the activated carbon at the reactor bed due to the Van der Walls force and releasing the heat due to exothermic reaction. This heat is called heat of adsorption. The contour of reactor bed can be seen with blue to the green colour indicating low pressure changes occur. As the process going to temperature 308K, more methane molecules being adsorbed by the activated carbon releasing large amount of heat and the contour colour of reactor bed change into yellowish to orange colour and this can be seen clearly at temperature 313K as the reactor bed turn into red contour indicating the highest pressure changes occur at the reactor bed. As for Design A, pressure distributions results show that Design A2 has the highest contour changes and while Design A3 has the lowest changes. Based on three sub-design for Design A, Design A2 has the lowest number of holes and small size of holes that allow methane gas flow inside the ANG tank compare to Design A1 and A3. On the other hand, Design A3 has the biggest size of holes that allow methane gas flow inside the ANG tank even though the number of holes is less. As for Design B, it has

found that the temperature distributions at reactor bed of Design B2 has the highest contour changes and while Design B3 has the lowest changes. Based on three sub-design for Design B, Design B2 has the lowest number of holes and small size of holes that allow methane gas flow inside the ANG tank compare to Design B1 and B3. On the other hand, Design B3 has the biggest size of holes that allow methane gas flow inside the ANG tank even though the number of holes is less. As for Design C, temperature distributions results show that Design C2 has the highest contour changes and while Design C3 has the lowest changes. Based on three sub-designs for Design C, Design C2 has the lowest number of holes and small size of holes that allow methane gas flow inside the ANG tank compare to Design C1 and C3. On the other hand, Design C3 has the biggest size of holes that allow methane gas flow inside the ANG tank even though the number of holes is less.. Based on these situations, it has been found that as the temperature of the bed increases the distribution of pressure contour also increase but depends on the size and amount of holes present at the reactor bed. As the size and number of holes decreases, the pressure variations increase. Apart from that, as the pressure increases, the rate o adsorption increases as the kinetic energy of the methane molecules increase. Thus more adsorption can occur. However, for ANG storage system to perform efficiently, the temperature must be kept at lower temperature since the adsorption rate decrease with increase of temperature.

Based on the findings in this study, the author has found that temperature and pressure distributions at reactor bed of ANG Storage System were affected by three main factors which are the total volume of reactor bed, the total surface area exposed to methane gas and the size of holes which allow methane gas to flow. These three factors will affect the pressure and temperature variations directly if it has been varied in this study. The total volume of reactor bed will be depends on the overall design that consist of activated carbon. As the total volume is higher, the capacity of the reactor bed to sustain heat of adsorption release is high compared to model that have less total volume where the heat distribution is faster throughout the design. It is important to ensure slower heat transfer along the reactor bed as the adsorption rate and capacity is affected directly based on the temperature. The next factor that has been identify can affect the pressure and temperature variation for reactor bed of ANG storage system is the total surface are exposed to methane gas. The principles

of ANG storage system rely on the ability of the pores of activated carbon which is the reactor bed to adsorb molecules of methane gas. As the amount of pores increases the amount of methane molecules adsorb also increases. Thus, by increasing the total surface area exposed to methane gas, the adsorption capacity can be increases. For this part, it is important to design type of reactor bed that has large total surface area. The last factor that has been identified by the author is the effect of size of holes which allow methane gas to flow. The reactor bed design has bulky volume and the methane gas can only diffuse by the outer surface only. By introducing the holes in the middle of the reactor bed can increase the rate of adsorption throughout the reactor bed thus reducing the charge time to store the gas. For this study, the author has varied the size and total number of holes to analyse the effects of introducing the hole to the pressure and temperature of reactor bed. As for temperature, as the size of holes and number of holes increases the temperature variations at the reactor bed change significantly while for the pressure is reduce. As the size and number of holes are reduced, it has been seen that the pressure variations at the reactor bed increases while the temperature decreases. This can relate back to the relationship of pressure and temperature with volume.

CHAPTER 6

CONCLUSION AND RECOMMENDATIONS

6.1 Conclusion

In conclusion, this research is a parametric study on Adsorbed Natural Gas Storage System that seems to have huge potential in transportation area and have been tipped as an alternative for Compressed Natural Gas and Liquefied Natural Gas. Using ANSYS FLUENT, the simulation was focused on the simulation on the reactor bed of ANG Storage Tank based on several designs that have been proposed. For this study, the main objectives were achieved as the author has proposed different designs to be analysed for the adsorption of methane gas and also to analyse the pressure and temperature variations at the reactor bed of ANG storage system.

Based on this study, the author has found that several conditions that will affect the ANG storage system. The most important principle is that as the temperature of the reactor increases the adsorption will be decrease. The second principle is as the pressure increases the adsorption rate will be increase with the consideration of temperature. On top of that, the author also found that there are three main factors that also can affect the temperature and pressure variations. These factors can be controlled in the designs approach for the reactor. The three factors involve are the total volume of reactor bed, the total surface area exposed to methane gas and the size of holes which allow methane gas to flow. However, this study only the beginning for the CFD simulation for ANG storage system and as far as the author concern, there are still many conditions and theory that can be used to simulate the ANG storage system

Last but not least, the author hopes that this study will give new insight for the development of ANG storage system in the future as for the time being, very few of the scholars have focusing on the CFD simulation of ANG storage system.

6.2 Recommendations

1. Analyse for full model to get more accurate result

This study practically used only quarter size from the full model. Since the CFD simulation for ANG storage system have not been done before, the author having difficulties in setting up the condition for the simulation. Due to time constraint, the author only manage to test for quarter model only since the simulation for full model will consume a lot of time and require super computer to ensure simulation can be done. Practically, the simulation for quarter model is not enough to get accurate result, but for this study can give insight for doing simulation in full model.

2. Check and analyse for other cell zones conditions

This study aim to simulate the reactor bed of ANG storage system without considering much on other cell zones such as the ANG tank and also the fluid which is the methane gas. This project is solely focusing on the pressure and temperature distribution at the bed of ANG storage system because it is the main component that needs to be controlled in order to get high performance of the system. For the time being, other cell zone is not being simulated since it will require more significant information that still uncertain. However, the author believes by involving the other two cell zone, it will affect the overall performance of the system.

3. Use different design for ANG tank

ANG tank used in this project is referred to benchmark design that was proposed by Rahman 2011 which used cylinder tank. Normally this type of design is used for the application of Compressed Natural Gas in Natural Gas Vehicle. Since ANG only operate at low pressure around 2-4 MPa, it is possible to used other type of design for the tank apart from using cylindrical shape. Theoretically by using different tank design, it could give different results especially in pressure variations.

4. Simulate for discharge cycle of ANG storage system

As a whole, Rahman 2011 also explained that ANG storage system can be divided into charge cycle and discharge cycle. Charge cycle is to store the methane gas inside the tank while discharge cycle is when the gas inside the tank is transfer out to be used in tertiary system such as combustion system in NGV. For this study, only charge cycle is being simulated by the author and check for the temperature and pressure variations at the reactor bed. The conditions for the discharge cycle is totally different from the charge cycle whereas during charge cycle the reactor bed need to be maintain at low temperature to enhance the adsorption while during discharge cycle the reactor bed need to be at high temperature to ensure the gas can be release from the Van der Walls force acting at the pores of the adsorbate.

5. Introduce circulating water to enhance heat transfer thus increase efficiency

Based on this study, the author has proved the theory of as the temperature increase, adsorption rate will decrease. In order for adsorption process to occur more efficient, the temperature of the reactor bed must be keep minimum to ensure more methane molecules can be adsorbed. Based on research by Rahman 2011, it has been proposed to introduce heat exchanger application at the reactor bed to control the temperature. The circulating water will reduce the temperature of reactor bed during charge cycle and it will increase the reactor bed temperature for discharge cycle. However, in order to simulate two systems at one model is very difficult to be done and need more research and time to generate the models.

6. Try to use other simulation software for example ANSYS CFX

In this project, the author has selected the software from ANSYS FLUENT to do the simulation for the ANG storage system. It has been proven by many scholars that this software is one of the best to simulate the fluid flow. However, this software cannot simulate the adsorption process that take place in ANG storage system and only simulate the heat transfer for the system. Basically the author used the value of heat of adsorption by the adsorption process to simulate the heat changes in the system. It would be better if the software can actually simulate the adsorption process that release

heat of adsorption and react with the reactor bed of the system. There are still many other software that can be used to simulate the fluid flow apart from ANSYS FLUENT.

7. Build prototype to compare the result

Nothing can be compared to the actual experiment that will produce the accurate result based on the conditions being applied. In order to validate the findings, by comparing the results of simulation and prototype will be the best approach. However it will consume huge amount of money and time to fabricate and run the experiments. The prototype basically can give more findings since it will work based on actual situation compared to the simulation that only produce the results based on the inputs that being inserted. For the simulation results will be better if there are details information provided.

REFERENCES

1) Perry, R. H. and Hilton, C. H.. 1974, *Chemical Engineers' Handbook*, 5th Edition, Chap. 9, p.12. McGraw-Hill, New York.

2) Emissions from the Combustion of Natural Gas, Retrieve June 25, 2013, from NaturalGas.org website: http://www.naturalgas.org/environment/naturalgas.asp .,

3) Rahman K. A., 2011, *"Experimental and Theoretical Studies On Adsorbed Natural Gas Storage System Using Activated Carbons"* (2011) :pg 4

4) Mota J. P. B., 1999, "Impact of gas composition on natural gas storage by adsorption," *International Chemical Engineering Journal* **45(5) :** 986-996.

5) Lozano-Castello, D., J. Alca˜niz-Monge, M.A. de la Casa-Lillo, D. Cazorla-Amor´os, and A. Linares-Solano, 2002, Fuel, 81, 1777–1803

6) Inomata, K., K. Kanazawa, Y. Urabe, H. Hosono, and T. Araki, 2002,. *Carbon* **40**, 87–93

7) Suzuki M., 1990, *Adsorption Engineering,* Tokyo, Japan, Kodansha Ltd.

8) Biloe, S., V. Goetz, and S. Mauran, 2001,. *AIChE Journal*, **47**, 2819–2830

9) Saha B. B., Koyama S., Ibrahim I. El-Sharkawy, Habib K., Srinivasan K., Dutta P., 2007, "Evaluation of adsorption parameters and heats of adsorption through desorption measurements," *Journal Chemical Engineering Dat)***, 52:** 2419-2424.

10) Brunauer S., Emmett P. H., Teller E., 1938, "Adsorption of gases in multimolecular layers," Journal of American Chemistry Society 60: 309-319.

11) Zainal M. F., 2012, *Modelling of Adsorbed Natural Gas (ANG) Storage System As An Alternative for Compressed Natural Gas (CNG) Storage System*

12) Slejko F. L., 1985, *Adsorption Technology: A step by step approach to process evaluation and application,* New York, Marcel Dekker, INC.

13) Ruthven, D.M., 1984, *Principles of Adsorption and Adsorption Processes*, John Wiley and Sons, London,

14) Rouquerol, F.; Rouquerol, J.; Sing, K., 1999, *Adsorption by Powders and Porous Solids: Principles, Methodology and Applications,* Academic Press, United Kingdom, pp.10-11, 18-20,

15) Do, D.D., 1998. Adsorption Analysis: Equilibria and Kinetics, Imperial College Press, Singapore,
16) Souza D. A., 2005, *"How To Understand Computational Fluid Dynamics Jargon"*, NAFEMS Ltd.

17) Bezzo F., Macchietto S., Pantelides C. C., 2000, "*A general framework for the integration of computational fluid dynamics and process simulation*", United Kingdom, Elsevier.

18) Ho Y. S., 2006. "Isotherm for the sorption of lead onto peat: Comparison of linear and non-linear methods," Polish Journal of environmental.Studies, Vol. 15, pp.81-86

19) Subramanyam B. and Das A., 2009. "Linearized and non-linearized isotherm models comparative study on adsorption of aqueous phenol solution in soil," Environ. Sci. Tech., Vol. 6, pp.633-640

20) Do D.D., 1998. Adsorption Analysis: Equilibria and Kinetics, Imperial College Press, London,

21) Inglezakis V.J., 2007, Solubility-normalized Dubinin–Astakhov adsorption isotherm for ion-exchange systems, Microporous and Mesoporous Materials, Volume 103, Issues 1–3, Pg 72–81, Elsevier.

22) Glueckauf, E., 1955. Theory of chromatography, Part 10: Formula for diffusion into spheres and their application to chromatography, Transactions of the Faraday Society, 51, pp.1540-1551,

23) Latham, J.L. and Burgess, A.E., 1981. Elementary Reaction Kinetics, Butterworth, London, pp.13-24,

24) Loh, W.S.; Rahman, K.A.; Saha, B.B.; Chakraborty, A.; Ng, K.C.; Chun, W.G.; 2010, Sorption Rate and Isotherms of Methane on Pitch-Based Activated Carbon using Volumetric Method, The 5th Asian Conference on Refrigeration and Airconditioning, Proceedings of 5th ACRA, June 7-9, Tokyo, Japan, Paper No. 051.

25) Al-Muhtaseb, S.A. and Ritter, J.A., 1999, Roles of surface heterogeneity and lateral interactions on the isosteric heat of adsorption and adsorbed phase heat capacity, Journal of Physical Chemistry B, 103, pp.2467-2479.

26) Myers, A.L., 2002, Thermodynamics of adsorption in porous materials, AIChE Journal, 48, pp.145-160